A small-molecule antagonist of the β-catenin/TCF4 interaction blocks the self-renewal of cancer stem cells and suppresses tumorigenesis

Fang, L., Zhu, Q., Neuenschwander, M., Specker, E., Wulf-Goldenberg, A., Weis, W.I., von Kries, J.P., Birchmeier, W.

Cancer Research
2016 FEB 15 ; 76(4): 891-901
doi: 10.1158/0008-5472.CAN-15-1519

Publisher: American Association for Cancer Research

A small-molecule antagonist of the β-catenin/TCF4 interaction blocks the self-renewal of cancer stem cells and suppresses tumorigenesis

Running title: Wnt inhibitor LF3

Liang Fang[1], Qionghua Zhu[1], Martin Neuenschwander[2], Edgar Specker[2], Annika Wulf-Goldenberg[3], William I. Weis[4], Jens P. von Kries[2] and Walter Birchmeier[1*]

Authors Affiliations: [1] Cancer Research Program, Max Delbrück Center for Molecular Medicine (MDC) in the Helmholtz Society, Berlin, Germany, [2] Screening Unit, Leibniz-Institut fuer Molekulare Pharmakologie, Berlin, Germany, [3] Experimental Pharmacology & Oncology (EPO), Berlin, Germany, and [4] Department of Structural Biology, Stanford University, Stanford, USA

***Corresponding author:** wbirch@mdc-berlin.de, phone: +49-30-9406-3800, fax: +49-30-9406-2656

Financial support: Supported by the German Research Foundation (DFG), grant FG806.

Disclosure of any potential Conflicts of Interest: The described chemical compounds may have commercial value.

Abstract

Wnt/β-catenin signaling is a highly conserved pathway essential for embryogenesis and tissue homeostasis. However, deregulation of this pathway can initiate and promote human malignancies, especially of the colon and head and neck. Therefore, Wnt/β-catenin signaling represents an attractive target for cancer therapy. We performed high-throughput screening (HTS) using AlphaScreen and ELISA techniques to identify small molecules that disrupt the critical interaction between β-catenin and the transcription factor TCF4 required for signal transduction. We found that compound LF3, a 4-thioureido-benzenesulfonamide derivative, robustly inhibited this interaction. Biochemical assays revealed clues that the core structure of LF3 was essential for inhibition. LF3 inhibited Wnt/β-catenin signals in cells with exogenous reporters and in colon cancer cells with endogenously high Wnt activity. LF3 also suppressed features of cancer cells related to Wnt signaling, including high cell motility, cell cycle progression, and the overexpression of Wnt target genes. However, LF3 did not cause cell death or interfere with cadherin-mediated cell-cell adhesion. Remarkably, the self-renewal capacity of cancer stem cells was blocked by LF3 in concentration-dependent manners, as examined by sphere formation of colon and head and neck cancer stem cells under non-adherent conditions. Finally, LF3 reduced tumor growth and induced differentiation in a mouse xenograft model of colon cancer. Collectively, our results strongly suggest that LF3 is a specific inhibitor of canonical Wnt signaling with anticancer activity that warrants further development for preclinical and clinical studies as a novel cancer therapy.

Introduction

Great efforts have been made over the past two decades to develop rational targeted cancer therapies, which are more effective than chemo- and radiotherapies and may cause fewer side effects. Successes involve drugs that act as tyrosine kinase inhibitors; to date, 28 such substances have been approved for clinical use (1). Drugs that interfere with other fundamental signaling systems, such as γ-secretase inhibitors that target Notch signals (2) or inhibitors that target Sonic hedgehog (3), have been developed and are being evaluated in preclinical and clinical trials. Other signaling systems whose deregulation is essential in the initiation and maintenance of cancers – such as Wnt/β-catenin signaling – need to be identified and targeted as means of expanding the current repertoire of anti-tumor strategies (4).

Wnt/β-catenin signaling is a system that is essential for embryonic development and tissue homeostasis that has been highly conserved throughout evolution (5-7). The key mediator of the pathway is β-catenin, a transcriptional co-activator whose level is tightly controlled by a multiprotein destruction complex in the cytoplasm. This complex is composed of Axin, adenomatous polyposis coli (APC), casein kinase 1α (CK1α), glycogen synthase kinase 3β (GSK3β) and β-transducin repeats containing protein (β-TrCP). The latter phosphorylate β-catenin and induce its ubiquitination and proteosomal degradation. Canonical Wnt ligands such as Wnt1 or Wnt3a stimulate the pathway by inhibiting the destruction complex; this results in the stabilization and nuclear translocation of β-catenin. There β-catenin interacts with members of the TCF/LEF family of transcription factors and recruits a

number of coactivators including B-cell lymphoma 9 (BCL9) and CREB-binding protein (CBP), ensuring efficient activation of Wnt target genes. A comprehensive list of Wnt target genes can be found at web.stanford.edu/group/nusselab/cgi-bin/wnt/.

The discovery of an association between β-catenin and the tumor suppressor gene APC led to the recognition of the essential role of Wnt/β-catenin signaling in various cancers (8-11). Aberrant Wnt signaling is frequently caused by mutations in APC, β-catenin and Axin2. A noted exception is melanoma, where activated Wnt/β-catenin signaling appears to be associated with reduced tumor formation (12). Deregulated Wnt signaling is not only important for cancer initiation, but is also crucial in late-stage cancers and in metastasis formation (13, 14). Recent studies have shown that cancer stem cells (CSCs) in various tumors exhibit deregulated Wnt/β-catenin signaling (15-17) and require higher Wnt activity than differentiated cancer cells to maintain their self-renewal and tumorigenic properties. This feature may be useful in specifically targeting cancer stem cells, a crucial factor in combatting cancer recurrence (18, 19).

Over the past decade, researchers in academia and industry have developed various strategies to identify small molecules that target components involved in Wnt signaling. Wnt inhibitors were initially identified through ELISA-based high Throughput Screening (HTS) of natural compounds that interfere with β-catenin/TCF4 interactions (20). Cell-based HTS has been applied to identify additional small-molecule inhibitors of the pathway, some of which target Wnt

secretion (the porcupine inhibitor IWP-2) (21) or the Wnt receptor complex (Dishevelled/Frizzled interaction inhibitors NSC668036 and FJ9) (22, 23). Other compounds have been found that enhance the stability of the β-catenin destruction complex (tankyrase inhibitors XAV939 and JW55) (24, 25) or disrupt the transcription complex (β-catenin/CBP interaction inhibitor ICG-001, β-catenin/TCF interaction inhibitors iCRT3 and CWP232228, and β-catenin/BCL9 interaction inhibitor carnosic acid) (26-29). These studies allowed the further development of small-molecule Wnt inhibitors that entered early clinical trials, including PRI-724, CWP232291 and LGK974 (30).

In human cancer, activating mutations of Wnt signaling components are frequently found at the level of the destruction or transcription complexes. We reasoned that efforts to develop new Wnt inhibitors could therefore be directed to the downstream components of the pathway, in particular to the β-catenin-TCF transcription complexes. This may require interference with protein-protein interactions, which is a challenging field of research (31). A further concern was the overlap of the binding sites of β-catenin with TCFs and E-cadherin, as seen in the structural analyses (32). Substances interfering with E-cadherin interaction could thus have opposing effects than interfering with Wnt signaling. We should however note that because of the much larger β-catenin/E-cadherin interaction surface, the K_d of this interaction can be 1000-fold lower than with the TCFs (33). β-Catenin/TCF4 interaction inhibitors have been recently described (27, 29), suggesting the great potential of such inhibitors to be developed for clinical use.

Here we took advantage of the AlphaScreen technology to perform HTS to identify small molecules that interfere with the interaction of β-catenin and TCF4. The compound LF3 was identified as a potent and specific inhibitor of activated Wnt/β-catenin signals in reporter cells, but it did not interfere with the interaction of β-catenin with E-cadherin. LF3 blocked properties related to Wnt addiction in colon cancer cells, including enhanced cell migration and the progression of the cell cycle, and interfered with the self-renewal of cancer stem cells. In a xenograft tumor model derived from colon cancer stem cells, LF3 did not only reduce tumor growth but also strongly induced tumor differentiation. We thus report on the discovery of a small-molecule Wnt inhibitor with promising chemical and biological properties, with a potential for further development into a lead compound for targeted therapies of Wnt-addicted tumors.

Materials and Methods

Cell culture

The cell lines HCT116, HCT15, HT29, SW480, SW620, LS174T, SW48, MCF7, Hela, HEK293 and MDCK were obtained from the ATCC and cultured in DMEM (Invitrogen) supplemented with 10% fetal bovine serum, penicillin and streptomycin. Mouse salivary gland cancer stem cells were isolated and cultured in DMEM/F12 (Invitrogen) supplemented with 20% KSR, nonessential minimal amino acids, penicillin, streptomycin, L-glutamine and β-mercaptoethanol. The cell identity was tested by PCR phenotyping for β-catenin and Bmpr1a (16).

Protein purification

The cDNA encoding residues 134-668 of human β-catenin were inserted into the pGEX-4-T1 vector (GE Healthcare), and the cDNA encoding residues 1-79 of human TCF4 were inserted into the pET-16b vector (Qiagen). A mutation of residue Asp16 of TCF4 was introduced by PCR mutagenesis with the primers: forward 5'-GACCTAGGCGCCAACGCCGAACTGATTTCCTTCA-3', and reverse 5'-TGAAGGAAATCAGTTCGGCGTTGGCGCCTAGGTC-3'. Recombinant fusion proteins were expressed in E. coli BL21 cells and purified through GSTrap FF or HisTrap FF columns (GE, details in Supplementary Materials and Methods). Biotinylated human TCF4 peptide (aa 8-53) was purchased from Biosyntan, Berlin, Germany.

Compound library, compound analogs, High Throughput AlphaScreen

A library containing 16671 World Drug Index-derived compounds was provided by ChemBioNet, designed by the drug design and modeling group of the Leibniz-Institut für Molekulare Pharmakologie, Berlin, Germany (34). Analogs of LF3 were purchased from ChemDiv (San Diego, CA) and ChemBridge (San Diego, CA) and dissolved in DMSO to a concentration of 50 mM. In the AlphaScreens, purified GST-hβ-catenin was first incubated with nickel chelate acceptor beads and His-hTCF4 incubated with glutathione donor beads (Perkinelmer) in PBS. They were then combined into 384-well AlphaPlates in the presence of 20 μM test compounds. Titration was used to determine the concentration of purified proteins used in the AlphaScreens, yielding signals in linear ranges. After 1 h incubation, protein-protein interactions induced luminescence, as measured by an EnVision multilabel plate reader (PerkinElmer, Waltham MA).

Sphere culturing of cancer stem cells

24-well cell culture plates were pre-coated with 250 μl polyhema (12 mg/ml in 95% ethanol, Sigma) to promote the growth of non-attached spheres. SW480 reporter cells and mouse salivary gland cancer stem cells were trypsinized and seeded as single cells into the sphere culture medium (F12:DMEM 1:1, 1X B-27 supplement, 20 ng/ml EGF, 20 ng/ml FGF, 0.5% methylcellulose) with or without treatment (16, 19). After 10 days, spheres were counted under a phase contrast microscope, and pictures were taken by AF6000 and DFC350FX (Leica).

Mouse xenografts and therapy with LF3

Unsorted GFP^{low} and GFP^{high} SW480 cells (1×10^4) were subcutaneously injected into the back skin of NOD/SCID mice. Tumor growth was monitored over a period of 45 days. For therapy, LF3 was administered *i.v.* at 50 mg/kg body weight for 3 rounds over 5 consecutive days, with 2-day breaks.

Gene expression profiling

After desired treatments, total RNA of salivary gland CSCs were extracted according to the standard TRIzol protocol (Invitrogen). RNA was purified with RNeasy kit (Qiagen) and prepared with TotalPrep RNA amplification kit (Illumina) for the microarray analysis using MouseRef-8 v2.0 expression beadchip Kit. Microarray data (GEO accession: GSE73732) were analyzed and exported with the software Genome Studio (Illumina). Pearson correlation was calculated with http://www.wessa.net/rwasp_correlation.wasp. Expression clustering was calculated and visualized with software Cluster and TreeView (Stanford University), respectively. Functional clustering of interesting genes was performed with http://david.abcc.ncifcrf.gov/.

The techniques ELISA, co-immunoprecipitation, Western blotting, the establishment of TOP-GFP reporter cell lines, Luciferase reporter assays, immunofluorescence, chromatin immunoprecipitation and gene transcription analyses with qRT-PCR, cell migration, proliferation with BrdU, cell death by apoptosis, cell cycle and cell surface marker analyses are described in Supplementary Materials and Methods.

Results

High Throughput Screening and biochemical characterization of small molecules that interfere with the interaction of β-catenin and TCF4

We performed AlphaScreen-based High Throughput Screenings (Fig. S1A (35)) with a library of 16,000 synthetic compounds (see Figure S1C) from the central open access technology platform of ChemBioNet (34), using a GST-tagged armadillo repeat domain of human β-catenin (GST-β-catenin, aa residues 134-668) and a His-tagged N-terminal region of human TCF4 (His-hTCF4, aa 1-79) (Fig. 1A (32, 36, 37), see Materials and Methods). The interaction between recombinant β-catenin and TCF4 was specific: in ELISA (Fig. S1B), binding could be inhibited by recombinant TCF4 (His-hTCF4) and an N-terminal peptide of TCF4 (Bio-TCFpeptide, aa 8-53), but not by TCF4 mutated at critical Asp16 (His-TCF4(D16A)) (32, 36, 37) or irrelevant proteins (Fig. S1C). From the primary AlphaScreens, compounds that inhibited interactions by at least 40% at 20 μM were selected, and false positives (which also appeared in non-related screens) were excluded (see the course of the screening procedure in Fig. S1D). 132 compounds were re-examined using both AlphaScreens and ELISAs, and finally 5 compounds were identified (termed LF1 to LF5) that inhibited interactions by 50% at concentrations below 10 μM in both assays (Fig. S1E,F). Due to its excellent chemical properties and expected plasma membrane permeability (predicted by Lipinski's rule (38)), compound LF3 (Fig. 1B, structure on the left) with an IC_{50} of less than 2 μM in both assays (Fig. 1B, right) was chosen for further studies.

To clarify the specific structural requirements of LF3, analogs were purchased and tested by ELISA. Deletion or replacement of the sulfonamide group (R1) by methyl, fluorine or nitro eliminated inhibitory activity (Fig. 1C). Deletion of the benzene tail (R2) strongly reduced activity (Fig. 1D). The distance between the benzene ring and core structure was also important; among the analogs with 2 or fewer methyl groups between the benzene and the core, only LF3h exhibited inhibitory activity as potent as that of LF3 in these biochemical experiments (Fig. 1D).

Compound LF3 interferes with the interaction of endogenous proteins in cells and inhibits Wnt/β-catenin signaling in cellular assays

To investigate the effects of LF3 on the interactions of endogenous cellular proteins, protein extracts from HCT116 cells were incubated with LF3 at 3.3 - 60 μM, and β-catenin together with its binding partners were pulled down by co-immunoprecipitation using specific anti-β-catenin antibodies. LF3 interfered with both β-catenin/TCF4 and β-catenin/LEF1 interactions in dose-dependent manners, as shown by Western blotting (Fig. 2A, quantification in B).

To evaluate biological activity, LF3 and analogs were examined for inhibition of Wnt/β-catenin signaling in stable HEK293 reporter cells that express GFP in a TCF/LEF-dependent fashion (TOP-GFP, SABiosciences). LF3 was the most potent inhibitor of TOP-GFP production with an IC_{50} of 22.2 ± 4.9 μM, when cells were stimulated with 3 μM of CHIR99021 (39), which is a GSK3β inhibitor and thus a Wnt activator (Fig. 2C,D). LF3h was less potent and was therefore not studied further. When compared with ICG-001 and XAV939, which are Wnt inhibitors that suppress Wnt signaling at the levels of nuclear

transcription and β-catenin destruction, respectively (scheme in Fig. S2A (25, 30)), LF3 inhibited TOP-GFP signals with kinetics and at levels comparable to ICG-001, but different from XAV939 (Fig. S2B). Conventional TOPflash assays in HeLa cells showed that LF3 inhibited luciferase signals with IC_{50} between 2.4 - 4.0 μM, which were stimulated by recombinant Wnt3a, CHIR99021 or overexpression of an activating β-catenin mutant (with four mutated N-terminal phosphorylation sites), but not by overexpression of a β-catenin/LEF1-HMG fusion protein (40), which has no interface for LF3 binding (Fig. 2E). LF3 did not significantly inhibit other reporters, i.e., Oct-Luciferase stimulated by Oct4, NF-κB-Luciferase by TNFα, or Notch-Luciferase by NICD (SABiosciences, Fig. 2F, Fig. S2C). These data indicate that the inhibition of canonical Wnt signaling by LF3 in cells is specific and may indeed occur downstream in the pathway, i.e., at the β-catenin/TCF4 level.

LF3 does not disturb E-cadherin-mediated cell adhesion

Both TCF4 and E-cadherin interact with β-catenin through common armadillo repeats (32, 41, 42); this was a major concern as we developed our inhibitor, since a loss of function of β-catenin in adherens junctions might increase cell migration and induce metastasis (43). We therefore examined whether LF3 might also disrupt the interaction between β-catenin and E-cadherin. Immunofluorescence staining of MDCK cells revealed that E-cadherin and β-catenin co-localized at cell-cell adhesion sites and showed merged cobblestone patterns (Fig. S2D; upper panel, Fig. S2H; left panel). This location was not altered by LF3 treatment, for instance at 60 μM, which however strongly disturbed Wnt/β-catenin signaling at this concentration (Fig.

S2D, middle panel; see also above). In contrast, treatment of cells with hepatocyte growth factor (HGF) at 40U/ml leads to scattering of cells, to the loss of cell-cell adhesions and to a relocation of E-cadherin and β-catenin to non-overlapping cytoplasmic sites (Fig. S2D, lower panel). When β-catenin was immunoprecipitated from protein extracts of HCT116 cells incubated with increasing concentrations of LF3 at 3.3 - 60 µM, the amount of E-cadherin bound to β-catenin remained unchanged (Fig. S2E, quantification in F). MDCK cells were also incubated with LF3 and subjected to trypsin treatment for 5 min, which largely digested E-cadherin and abrogated E-cadherin-mediated cell-cell adhesion (Fig. S2G, Fig. S2H; 2nd panel). After removing the trypsin, cells were allowed to reform E-cadherin/β-catenin complexes at cell-cell adhesions: in the presence of LF3, the time-course of recovery of E-cadherin/β-catenin-mediated cell-cell adhesion was as in controls (Fig. S2H, 3rd - 5th panel). Overall, these data show that LF3 inhibits Wnt/β-catenin signaling, but does not interfere with E-cadherin/β-catenin-mediated cell-cell adhesion.

LF3 inhibits Wnt/β-catenin target gene expression and impairs Wnt-associated properties of colon cancer cells

In colon cancer cells that harbor Wnt/β-catenin-activating mutations, the Wnt target genes *Axin2* and *c-Myc* are actively transcribed upon binding of β-catenin/TCF4 to their promoter regions. Sequences near the promoters of *Axin2* and *c-Myc* were enriched by anti-β-catenin chromatin immunoprecipitation (ChIP) from HCT116 cells, and the enrichments were significantly reduced by LF3 at 30 µM (Fig. 3A). As shown by qRT-PCR, LF3

at 10 - 60 μM also inhibited the expression of many Wnt target genes (*Bmp4, Axin2, Survivin, c-Myc*, *Bambi* and *c-Myc)* in a dosage-dependent manner (Fig. 3B); ICG-001 at 25 μM or siRNA treatment against β-catenin had similar effects. The production of Axin2, c-Myc and cyclinD1 proteins was also suppressed by LF3 at 30 μM in a panel of colon cancer cell lines (Fig. 3C-F, Fig. S3A-H). Thus, LF3 blocks the expression of a series of Wnt target genes in Wnt-addicted colon cancer cells.

Wnt/β-catenin signaling contributes to high cell motility, high cell proliferation and cell cycle progression in colon cancer cells. Boyden chamber motility assays with SW480 colon cancer cells showed that LF3 at 10 and 30 μM strongly reduced cell migration in a dosage-dependent manner (Fig. 4A). LF3 at 30 and 60 μM also reduced proliferation, as measured by BrdU-incorporation, in the Wnt-dependent colon cancer cell lines HCT116 and HT29, but not in the Wnt-independent breast cancer cell line MCF7 (Fig. 4B). Cleaved caspase3 and propidium iodide staining indicated that the inhibition of proliferation, for instance in HCT116 cells, was not due to apoptotic or cytotoxic effects of LF3 at 60 μM, which are induced in cells by puromycin at 1 μg/ml (Fig. S4A,B). Instead, we observed that LF3 at 30 and 60 μM induced cell cycle arrest in the G1 phase of HCT116 and HT29 cells in dosage-dependent manners (Fig. 4C), but had only an insignificant influence on the cell cycle of MCF7 cells. These data show that LF3 inhibits proliferation of Wnt-addicted colon cancer cells through induction of cell cycle arrest.

LF3 inhibits the self-renewal capacity of cancer stem cells

It has been reported that high Wnt/β-catenin activity characterizes colon cancer stem cells and other cancer stem cells, which are fractions of tumor cells capable of regenerating entire tumors following transplantation (18, 19, 44). A small molecule Wnt inhibitor CWP232228 has recently been shown to be able to inhibit the proliferation of breast cancer stem cells (29). Stem and cancer stem cells are generally enriched in non-attached sphere cultures, which reflect their self-renewal capacity (45, 46). We asked whether LF3 could specifically target colon and salivary gland cancer stem cells through Wnt/β-catenin inhibition. A reporter cell line that expressed TOP-GFP (see above) was generated from SW480 colon cancer cells. Flow cytometry analysis revealed heterogeneous expression of GFP in this cell line (Fig. 5A). GFP intensity correlated with Wnt/β-catenin activity, as shown by upregulated mRNA and protein levels of Wnt target genes (*Bmp4, Lgr5, Vimentin, Axin2, Bambi* and *Lef1)* in the GFP^{high2} population, compared to the GFP^{low2} population (Fig. 5B,C). Immunofluorescence revealed intense nuclear β-catenin staining in the GFP^{high2} population, while E-cadherin staining at cell borders was strongly reduced (Fig. 5D, lower panel). In GFP^{low2} cells, E-cadherin was homogeneously high and β-catenin was low, while unsorted cells showed separated sub-clones of the different cell subpopulations (Fig. 5D, middle and upper panels, respectively). The expression of the human stem cell markers CD44 and CD29 also correlated with Wnt/β-catenin activity; the fraction of $CD44^{high}CD29^{+}$ cells increased from 20% in the GFP^{low1} population to 91% in the GFP^{high2} population (Fig. S5A,B). Cells from different subpopulations were then cultured under anchorage-independent conditions

in serum-free medium to test their sphere-forming ability in the absence or presence of LF3 at 10 and 30 μM. All 4 cell populations formed spheres, but GFP^{high} populations formed significantly more spheres than GFP^{low} populations (Fig. 5E,F), expressed TOP-GFP, and they were larger (Fig. 5E, 3rd panel). Remarkably, treatment with LF3 reduced the number and size of spheres formed from GFP^{high} populations, but had no significant impact on GFP^{low} cells (Fig. 5E,F). In sequential rounds of colony assays, GFP^{high} cells produced similarly high number of spheres in each passage, but in the presence of LF3 sphere numbers were reduced continually (Fig. S5C).

We had found previously that salivary gland squamous cell carcinomas were generated in mice that harbor β-catenin gain-of-function ($\beta\text{-cat}^{GOF}$) and Bmp receptor 1a loss-of-function ($Bmpr1a^{LOF}$) mutations driven by Keratin14-Cre recombinase (Fig. 6A (16)). A $CD24^{high}CD29^{+}$ cell population (Fig. 6B, encircled in red in the left panel and following purification in the right panel) was characterized as salivary gland cancer stem cells by their potent sphere-forming capacity in culture and their high tumorigenic potential following transplantation (16). Remarkably, the expression of stem cell-associated, chromatin modifier and Wnt target genes that are highly expressed in the salivary gland cancer stem cells were downregulated by LF3 at 30 μM, by ICG-001 at 25 μM, by the recently identified new Wnt inhibitor iCRT3 (27) at 60 μM, and by β-catenin siRNA (Fig. 6C). LF3 also inhibited proliferation and sphere formation of these cells in dosage-dependent manners, as did ICG-001 (Fig. 6D-F). Similarly, treatment with LF3 or ICG-001 induced differentiation of salivary gland cancer stem cells, as indicated by up-

regulated expression of Amylase1, CA6 and Loricrin, and formation of hollow spheres in 3D matrigel culture (Fig. 6G, Fig. S6A,B) (16, 17).

We also investigated Wnt/β-catenin target genes using gene expression profiling in salivary gland cancer stem cells treated with LF3 or ICG-001, since these inhibitors affect canonical Wnt signaling through different mechanisms, e.g., by inhibition of β-catenin-TCF/LEF1 and β-catenin-CBP interactions, respectively in this study (30). Several canonical Wnt target genes including *Vimentin, Ephb2, Ash2l, Birc5* and *Id2* were downregulated by both LF3 and ICG-001 (Fig. S6C). Overall, a majority of 325 genes (72.5%) were downregulated by both LF3 and ICG-001 (Fig. S6D), giving a high Pearson correlation coefficient of 0.73 (Fig. S6E). Gene clustering identified genes that were similarly or differentially regulated by LF3 and ICG-001 (Fig. S6F). Then a functional clustering of genes from the different groups was performed using DAVID bioinformatics resources. Genes that are involved in essential cellular processes such as cell cycle progression, macromolecular metabolism, transcription regulation, and others were similarly regulated by LF3 and ICG-001 (Fig. S6F). Two clusters of genes which contribute to metal ion-binding and purine nucleotide-binding were differentially regulated by the two inhibitors, respectively (Table S3).

LF3 reduces tumor growth and induces tumor differentiation

To examine the effects of LF3 on tumor formation, GFP^{high} and GFP^{low} SW480 cells (see Fig. 5A) were injected subcutaneously into the back skin of NOD/SCID mice (1×10^4 cells per mouse). Within 40 days, all mice injected with GFP^{high} cells developed tumors, whereas only one out of five mice

injected with GFP^{low} cells developed a tumor (Fig. 7A). When mice with GFP^{high} cells were treated with LF3 at 50mg/kg through systemic *i.v.* injection for 3 weeks before tumor formation, tumor growth was significantly reduced (Fig. 7B, Fig. S7A). Inhibition was also observed, when treatment was started after tumors were palpable (Fig. S7B). No systemic toxicity, e.g., by weight loss was observed in the treated mice (Fig. S7C). Immunofluorescence showed that tumors induced by GFP^{high} cells exhibited undifferentiated features including high expression of Lef-1 or Vimentin, nuclear location of β-catenin and loss of E-cadherin, Keratin20 and Muc2 (Fig. 7C, Fig. S7D, upper panel). Remarkably, LF3-treated tumors became highly differentiated, as shown by expression of high E-cadherin, Keratin20 and Muc2, by membrane localization of β-catenin and by down-regulation of Lef-1 and Vimentin (Fig. 7C, Fig. S7D, lower panel, quantified in Fig. 7D, Fig. S7E). LF3 treatment did not disturb the normal histology of the gut of mice (Fig. S7F). These data show that LF3 has potent tumor inhibition and differentiation capacities in xenotransplanted tumors.

Discussion

Wnt signaling's crucial role in cancer biology has made it an important target to pursue in the development of new therapeutic strategies. So far, however, few rationally designed Wnt inhibitors have entered clinical trials, and of those being tried, some target Wnt ligand secretion or receptor binding (reviewed in (30)). In the present study, we focused on inhibiting the interaction between β-catenin and TCF4, with the goal of overcoming deregulations of Wnt signaling caused by mutations of components that lie upstream in the pathway. The small molecule LF3 was identified in a biochemical screen using purified recombinant interaction partners. By specifically inhibiting the β-catenin/TCF4 interaction, LF3 diminished Wnt-dependent biological characteristics of colon cancer cells including high proliferation and high motility. Remarkably, LF3 also inhibited the self-renewal capacity of human colon and mouse salivary gland cancer cells and induced their differentiation.

By comparing gene expression profiles of mouse salivary gland CSCs treated with LF3 or ICG-001, two compounds that target the transcription complexes at different positions, we observed a large overlap in dis-regulated genes, including well-known Wnt targets. This was surprising given the fact that the ICG-001 target CBP is known to interact with numerous transcription factors and can thus regulate many signaling systems (47). LF3 and ICG-001 apparently inhibit deregulated Wnt signaling with a similar overall outcome. Further investigations are needed to understand whether the small sets of genes regulated by either TCF4 or CBP are critical for specific CSCs and tumors. Moreover, we show that the potency of LF3 is comparable with ICG-

001 or iCRT3. LF3 at 50 mg/kg significantly reduced the growth of colon cancer stem cells during tumor formation while exhibiting no significant toxicity for mice. These results suggest that LF3 has the potential for further development with the aim of preclinical and clinical trials.

Drug development, especially downstream in Wnt signaling, faces the challenge of finding inhibitors that target specific protein-protein interactions. Yet there is increasing evidence that small molecules that effectively dock onto hotspots of the interaction sites between partners and thus inhibit their interactions can indeed be found (reviewed in (48)). Such hotspots have been reported for the β-catenin/TCF4 interaction (32, 37). Efforts have been made to identify such inhibitors using, for instance, the compounds PKF115-584, CGP049090, PNU-74654 and iCRTs (20, 27, 49). In the present study, advanced biochemical screening techniques and the use of in-house synthetic compound libraries allowed us to identify compound LF3. The mechanistic details of the way LF3 disrupts β-catenin/TCF4 interaction remain to be shown; a strong hypothesis is that the negatively charged sulfonamide group of LF3 may compete with Asp16 of TCF4 to bind to the positively charged pocket of β-catenin formed by Lys435. The hydrophobic tail of LF3 might insert itself into a hydrophobic cleft lined by the residues Cys466 and Pro463 of β-catenin to facilitate interaction (32, 37). Solving the structure of LF3 with the partner proteins will help answer these questions and will also permit medicinal chemistry approaches to be applied to improve the activity of the compound.

Cancer stem cells are implicated in therapy resistance, metastasis formation and cancer relapse (50). In various cancers, CSCs are maintained by single signaling systems or by combinations of systems. If these are inhibited,

tumors may be forced to differentiate, as we have shown here in transplanted colon cancer cells. By inhibiting Wnt signaling, LF3 blocks the self-renewal of Wnt-high CSCs and induces their differentiation both *in vitro* and in xeno-transplants. Remarkably, the population of Wnt-low cells in SW480 cells did not response to LF3 treatment. These cells appear to be supported by other signaling systems and driver mutations. Tumors that exhibit complex cellular heterogeneity may include different CSC populations supported by different signaling systems, and thus a combination of targeted therapies may be required to treat these cases in a personalized way.

References

1. Wu P, Nielsen TE, Clausen MH. FDA-approved small-molecule kinase inhibitors. Trends Pharmacol Sci. 2015;36:422-39.

2. Groth C, Fortini ME. Therapeutic approaches to modulating Notch signaling: current challenges and future prospects. Semin Cell Dev Biol. 2012;23:465-72.

3. Basset-Seguin N, Sharpe HJ, de Sauvage FJ. Efficacy of Hedgehog Pathway Inhibitors in Basal Cell Carcinoma. Mol Cancer Ther. 2015.

4. Polakis P. Drugging Wnt signalling in cancer. Embo J. 2012;31:2737-46.

5. Logan CY, Nusse R. The Wnt signaling pathway in development and disease. Annual review of cell and developmental biology. 2004;20:781-810.

6. Grigoryan T, Wend P, Klaus A, Birchmeier W. Deciphering the function of canonical Wnt signals in development and disease: conditional loss- and gain-of-function mutations of beta-catenin in mice. Genes & development. 2008;22:2308-41.

7. Clevers H. Wnt/beta-catenin signaling in development and disease. Cell. 2006;127:469-80.

8. de Lau W, Barker N, Clevers H. WNT signaling in the normal intestine and colorectal cancer. Front Biosci. 2007;12:471-91.

9. Tennis M, Van Scoyk M, Winn RA. Role of the wnt signaling pathway and lung cancer. J Thorac Oncol. 2007;2:889-92.

10. Robinson DR, Zylstra CR, Williams BO. Wnt signaling and prostate cancer. Current drug targets. 2008;9:571-80.

11. Takigawa Y, Brown AM. Wnt signaling in liver cancer. Current drug targets. 2008;9:1013-24.

12. Chien AJ, Moore EC, Lonsdorf AS, Kulikauskas RM, Rothberg BG, Berger AJ, et al. Activated Wnt/beta-catenin signaling in melanoma is associated with decreased proliferation in patient tumors and a murine melanoma model. Proc Natl Acad Sci U S A. 2009;106:1193-8.

13. Stein U, Arlt F, Walther W, Smith J, Waldman T, Harris ED, et al. The metastasis-associated gene S100A4 is a novel target of beta-catenin/T-cell factor signaling in colon cancer. Gastroenterology. 2006;131:1486-500.

14. Nguyen DX, Chiang AC, Zhang XH, Kim JY, Kris MG, Ladanyi M, et al. WNT/TCF signaling through LEF1 and HOXB9 mediates lung adenocarcinoma metastasis. Cell. 2009;138:51-62.

15. Barker N, Ridgway RA, van Es JH, van de Wetering M, Begthel H, van den Born M, et al. Crypt stem cells as the cells-of-origin of intestinal cancer. Nature. 2009;457:608-11.

16. Wend P, Fang L, Zhu Q, Schipper JH, Loddenkemper C, Kosel F, et al. Wnt/beta-catenin signalling induces MLL to create epigenetic changes in salivary gland tumours. Embo J. 2013;32:1977-89.

17. Holland JD, Gyorffy B, Vogel R, Eckert K, Valenti G, Fang L, et al. Combined Wnt/beta-Catenin, Met, and CXCL12/CXCR4 Signals Characterize Basal Breast Cancer and Predict Disease Outcome. Cell Rep. 2013.

18. Malanchi I, Peinado H, Kassen D, Hussenet T, Metzger D, Chambon P, et al. Cutaneous cancer stem cell maintenance is dependent on beta-catenin signalling. Nature. 2008;452:650-3.

19. Vermeulen L, De Sousa EMF, van der Heijden M, Cameron K, de Jong JH, Borovski T, et al. Wnt activity defines colon cancer stem cells and is regulated by the microenvironment. Nature cell biology. 2010;12:468-76.

20. Lepourcelet M, Chen YN, France DS, Wang H, Crews P, Petersen F, et al. Small-molecule antagonists of the oncogenic Tcf/beta-catenin protein complex. Cancer cell. 2004;5:91-102.

21. Chen B, Dodge ME, Tang W, Lu J, Ma Z, Fan CW, et al. Small molecule-mediated disruption of Wnt-dependent signaling in tissue regeneration and cancer. Nature chemical biology. 2009;5:100-7.

22. Shan J, Shi DL, Wang J, Zheng J. Identification of a specific inhibitor of the dishevelled PDZ domain. Biochemistry. 2005;44:15495-503.

23. Grandy D, Shan J, Zhang X, Rao S, Akunuru S, Li H, et al. Discovery and characterization of a small molecule inhibitor of the PDZ domain of dishevelled. J Biol Chem. 2009;284:16256-63.

24. Waaler J, Machon O, Tumova L, Dinh H, Korinek V, Wilson SR, et al. A novel tankyrase inhibitor decreases canonical Wnt signaling in colon carcinoma cells and reduces tumor growth in conditional APC mutant mice. Cancer Res. 2012;72:2822-32.

25. Huang SM, Mishina YM, Liu S, Cheung A, Stegmeier F, Michaud GA, et al. Tankyrase inhibition stabilizes axin and antagonizes Wnt signalling. Nature. 2009;461:614-20.

26. Eguchi M, Nguyen C, Lee SC, Kahn M. ICG-001, a novel small molecule regulator of TCF/beta-catenin transcription. Medicinal chemistry (Shariqah (United Arab Emirates)). 2005;1:467-72.

27. Gonsalves FC, Klein K, Carson BB, Katz S, Ekas LA, Evans S, et al. An RNAi-based chemical genetic screen identifies three small-molecule inhibitors of the Wnt/wingless signaling pathway. Proc Natl Acad Sci U S A. 2011;108:5954-63.

28. de la Roche M, Rutherford TJ, Gupta D, Veprintsev DB, Saxty B, Freund SM, et al. An intrinsically labile alpha-helix abutting the BCL9-binding site of beta-catenin is required for its inhibition by carnosic acid. Nat Commun. 2012;3:680.

29. Jang GB, Hong IS, Kim RJ, Lee SY, Park SJ, Lee ES, et al. Wnt/beta-Catenin Small-Molecule Inhibitor CWP232228 Preferentially Inhibits the Growth of Breast Cancer Stem-like Cells. Cancer research. 2015;75:1691-702.

30. Kahn M. Can we safely target the WNT pathway? Nat Rev Drug Discov. 2014;13:513-32.

31. Wells JA, McClendon CL. Reaching for high-hanging fruit in drug discovery at protein-protein interfaces. Nature. 2007;450:1001-9.

32. von Kries JP, Winbeck G, Asbrand C, Schwarz-Romond T, Sochnikova N, Dell'Oro A, et al. Hot spots in beta-catenin for interactions with LEF-1, conductin and APC. Nature structural biology. 2000;7:800-7.

33. Choi HJ, Huber AH, Weis WI. Thermodynamics of beta-catenin-ligand interactions: the roles of the N- and C-terminal tails in modulating binding affinity. J Biol Chem. 2006;281:1027-38.

34. Lisurek M, Rupp B, Wichard J, Neuenschwander M, von Kries JP, Frank R, et al. Design of chemical libraries with potentially bioactive molecules applying a maximum common substructure concept. Mol Divers. 2010;14:401-8.

35. Eglen RM, Reisine T, Roby P, Rouleau N, Illy C, Bosse R, et al. The use of AlphaScreen technology in HTS: current status. Curr Chem Genomics. 2008;1:2-10.

36. Omer CA, Miller PJ, Diehl RE, Kral AM. Identification of Tcf4 residues involved in high-affinity beta-catenin binding. Biochem Biophys Res Commun. 1999;256:584-90.

37. Fasolini M, Wu XQ, Flocco M, Trosset JY, Oppermann U, Knapp S. Hot spots in Tcf4 for the interaction with beta-catenin. Journal of Biological Chemistry. 2003;278:21092-8.

38. Lipinski CA, Lombardo F, Dominy BW, Feeney PJ. Experimental and computational approaches to estimate solubility and permeability in drug discovery and development settings. Adv Drug Deliv Rev. 2001;46:3-26.

39. Sineva GS, Pospelov VA. Inhibition of GSK3beta enhances both adhesive and signalling activities of beta-catenin in mouse embryonic stem cells. Biology of the cell / under the auspices of the European Cell Biology Organization. 2010;102:549-60.

40. Wong MH, Huelsken J, Birchmeier W, Gordon JI. Selection of multipotent stem cells during morphogenesis of small intestinal crypts of Lieberkuhn is perturbed by stimulation of Lef-1/beta-catenin signaling. The Journal of biological chemistry. 2002;277:15843-50.

41. Hulsken J, Birchmeier W, Behrens J. E-cadherin and APC compete for the interaction with beta-catenin and the cytoskeleton. The Journal of cell biology. 1994;127:2061-9.

42. Pai LM, Kirkpatrick C, Blanton J, Oda H, Takeichi M, Peifer M. Drosophila alpha-catenin and E-cadherin bind to distinct regions of Drosophila Armadillo. J Biol Chem. 1996;271:32411-20.

43. Birchmeier W, Behrens J. Cadherin expression in carcinomas: role in the formation of cell junctions and the prevention of invasiveness. Biochim Biophys Acta. 1994;1198:11-26.

44. Lukacs RU, Memarzadeh S, Wu H, Witte ON. Bmi-1 is a crucial regulator of prostate stem cell self-renewal and malignant transformation. Cell Stem Cell. 2010;7:682-93.

45. Wend P, Holland JD, Ziebold U, Birchmeier W. Wnt signaling in stem and cancer stem cells. Semin Cell Dev Biol. 2010;21:855-63.

46. Holland JD, Klaus A, Garratt AN, Birchmeier W. Wnt signaling in stem and cancer stem cells. Curr Opin Cell Biol. 2013;25:254-64.

47. Vo N, Goodman RH. CREB-binding protein and p300 in transcriptional regulation. The Journal of biological chemistry. 2001;276:13505-8.

48. Jin L, Wang W, Fang G. Targeting protein-protein interaction by small molecules. Annu Rev Pharmacol Toxicol. 2014;54:435-56.

49. Trosset JY, Dalvit C, Knapp S, Fasolini M, Veronesi M, Mantegani S, et al. Inhibition of protein-protein interactions: the discovery of druglike beta-catenin inhibitors by combining virtual and biophysical screening. Proteins. 2006;64:60-7.

50. Li F, Tiede B, Massague J, Kang Y. Beyond tumorigenesis: cancer stem cells in metastasis. Cell Res. 2007;17:3-14.

Figure legends

Figure 1 Compound LF3 disrupts the interaction between β-catenin and TCF4. (A) GST-tagged armadillo domain of β-catenin and His-tagged and biotinylated N-terminal region of TCF4 were prepared for AlphaScreen-based High Throughput Screening and ELISA to identify and verify compounds that disrupt the interaction between β-catenin and TCF4. (B) LF3 (structure and characteristics on the left) inhibits β-catenin/TCF4 interaction in both AlphaScreen and ELISA with IC50 of 1.65 and 1.82 μM, respectively. (C,D) Analogs of LF3 were tested in ELISA for their ability to inhibit β-catenin/TCF4 interaction. Among all the analogs tested, LF3e and LF3g interfered with the interaction mildly, and only LF3h had an IC50 value comparable to LF3.

Figure 2 LF3 specifically inhibits Wnt/β-catenin signaling in cells. (A,B) β-catenin was immunoprecipitated from protein extracts of HCT116 cells that were incubated with LF3 at increasing concentrations, and reduced TCF4 and LEF1 bound to β-catenin were shown by Western blotting. (C,D) TOP-GFP reporter cells were incubated with 3 μM CHIR99021 and with LF3, LF3h or LF3i at increasing concentrations. After 24 h, reduced GFP intensity was observed in LF3-treated cells. Compared to LF3h and LF3i, LF3 showed the most potent inhibition of Wnt signaling. (E) Hela cells were co-transfected with TOPflash-Luc plasmid (Wnt reporter) and pRL-SV40 plasmid (control for transfection), and stimulated with mWnt3a, CHIR99021, β-catenin activating mutant or β-catenin-Lef1 fusion in the presence or absence of LF3. LF3 inhibited Wnt/β-catenin activation induced by mWnt3a, CHIR99021, β-catenin mutant, but not by β-catenin-Lef1. (F) The pRL-SV40 plasmid was co-

transfected with different reporter plasmids including Oct-Luc, NF-κB-Luc or Notch-Luc into Hela cells. Different reporter activity was stimulated with specific treatments in the presence or absence of LF3. Compared to the inhibitory effect on the Wnt reporter, LF3 had no or very mild effects on other reporters.

Figure 3 LF3 inhibits Wnt/β-catenin signaling in colon cancer cells. (A) HCT116 cells were incubated with 30 μM LF3 for 4 h and then cross-linked to immunoprecipitate β-catenin with bound DNA fragments. Reduced association of β-catenin with the Axin2 and c-Myc promoters by LF3 was shown by using specific primer pairs recognizing β-catenin binding-regions on the promoters by quantitative real-time PCR. (B) HCT116 cells were treated with various concentrations of LF3, 25 μM ICG-001 (for 24 h) or siβ-catenin (for 48 h), and downregulated mRNA levels of Wnt target genes were measured by quantitative real-time PCR. The effect of LF3 was comparable to ICG-001 and siβ-catenin treatment. (C,D,E,F) HCT116 (C,D) and SW480 (E,F) cells harboring different mutations in Wnt components were treated with LF3 for 24 h. Downregulation of Wnt targets at the protein level was demonstrated by Western blotting (C,E; quantitation is in D,F).

Figure 4 LF3 affects cell migration, proliferation and cell cycle progression of colon cancer cells. (A) SW480 cells were cultured with or without LF3 in the upper chambers of transwells, and stimulated to migrate by fetal bovine serum into the lower chambers. Reduced migration of SW480 cells was observed after 24 h treatment of LF3. (B) Two colon cancer cell lines (HCT116 and HT29) and a breast cancer cell line (MCF7) were treated

with LF3 for 24 h and labeled with BrdU for 4 - 5 h to detect proliferating cells. BrdU-labeled cells were reduced upon LF3 treatment of colon cancer cells lines but not of MCF7 cells. (C) HCT116, HT29 and MCF7 cells were treated with LF3 for 24 h and fixed to analyze their cell cycle distribution. LF3 increased cell numbers in the G1 and G2/M phases in HCT116 and HT29 cells but not in MCF7 cells.

Figure 5 LF3 inhibits the self-renewal of colon CSCs. (A) SW480 cells were stably transfected by the TOP-GFP reporter and analyzed for GFP expression by FACS. A heterogeneous GFP expression was observed in SW480 cells. (B) Different populations of cells were analyzed by real-time PCR for their mRNA levels of Wnt/β-catenin targets. Compared with SW480-unsorted and GFP^{low} populations, the GFP^{high} population showed much higher transcription of Wnt targets. (C,D) Immunofluorescence and Western blotting were used to detect protein levels of Wnt-controlled proteins in different cell populations. Compared with GFP^{low} cells, GFP^{high} cells expressed high levels of β-catenin and Wnt target genes and low levels of E-cadherin. Nuclear localization of β-catenin was observed in GFP^{high} cells. (E,F) Different populations of SW480 cells were cultured in non-adherent conditions with or without LF3 to test their ability to form spheres and the influence of LF3. GFP^{high} populations formed more and larger spheres expressing GFP than GFP^{low} populations. LF3 reduced the number and the size of spheres formed from GFP^{high} populations, but had no effect on the number and a very mild effect on the size of spheres formed from the GFP^{low} populations.

Figure 6 LF3 induces differentiation of mouse salivary gland CSCs. (A) Exon3 of β-catenin and exon2 of Bmpr1a, flanked by loxP sites, were deleted by Keratin14-Cre recombinase, resulting in salivary gland tumors with β-catenin gain-of-function and Bmp receptor 1a loss-of-function mutations. (B) Based on surface marker expression, salivary gland CSCs ($CD24^{high}CD29^{+}$ cells) can be isolated from salivary gland tumors and cultured. (C) CSCs were treated with different Wnt inhibitors (for 24 h) and siβ-catenin (for 48 h), and mRNA levels of various genes were measured with quantitative real-time PCR. LF3 inhibited the transcription of Wnt target genes and genes that are important for keeping the stemness of CSCs, including stem cell signature genes and chromatin modifier genes, as efficiently as the other inhibitors. (D,E,F) Salivary gland CSCs were either cultured in adherent conditions to observe proliferation or in non-adherent conditions to observe self-renewal in the presence or absence of LF3 and ICG-001. LF3 dose-dependently inhibited proliferation and sphere formation of salivary gland CSCs, and the concentrations required of LF3 were comparable with those of ICG-001. (G) The differentiation marker Amylase1 of salivary gland CSCs was analyzed after treatment with LF3 or ICG-001. Both inhibitors induced the upregulation of Amy1.

Figure 7 LF3 reduces tumor growth and induces differentiation of colon CSCs in vivo. (A) Tumor-free survival of NOD/SCID mice that were injected subcutaneously with unsorted, GFP^{low} and GFP^{high} SW480 cells (1×10^4 cells per mouse). All mice (5/5) with GFP^{high} cells, 4/5 mice with unsorted cells and 1/5 mice with GFP^{low} cells developed tumors. (B) Mice xenografted with GFP^{high} SW480 cells were treated *i.v.* with vehicle (n=10) or 50mg/kg LF3

(n=6) for 3 weeks, and tumor volumes were monitored over time. (C,D) Histological changes and expression changes of Lef1, Vimentin and E-cadherin in LF3-treated tumors were demonstrated by H&E-staining and immunofluorescence. LF3 down-regulated the expression of Lef1 and Vimentin, and up-regulated E-cadherin. 10 tumors from the vehicle group and 6 tumors from the LF3 group were evaluated.

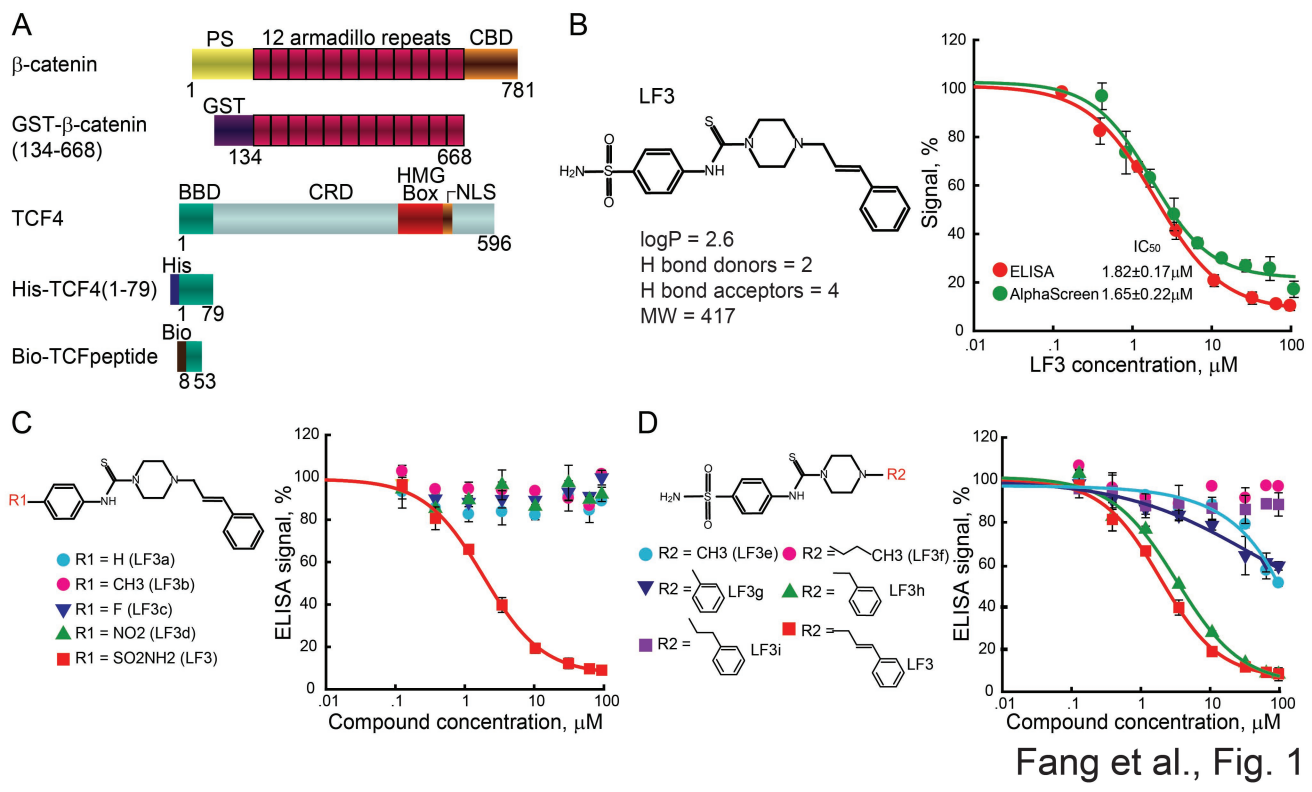

Fang et al., Fig. 1

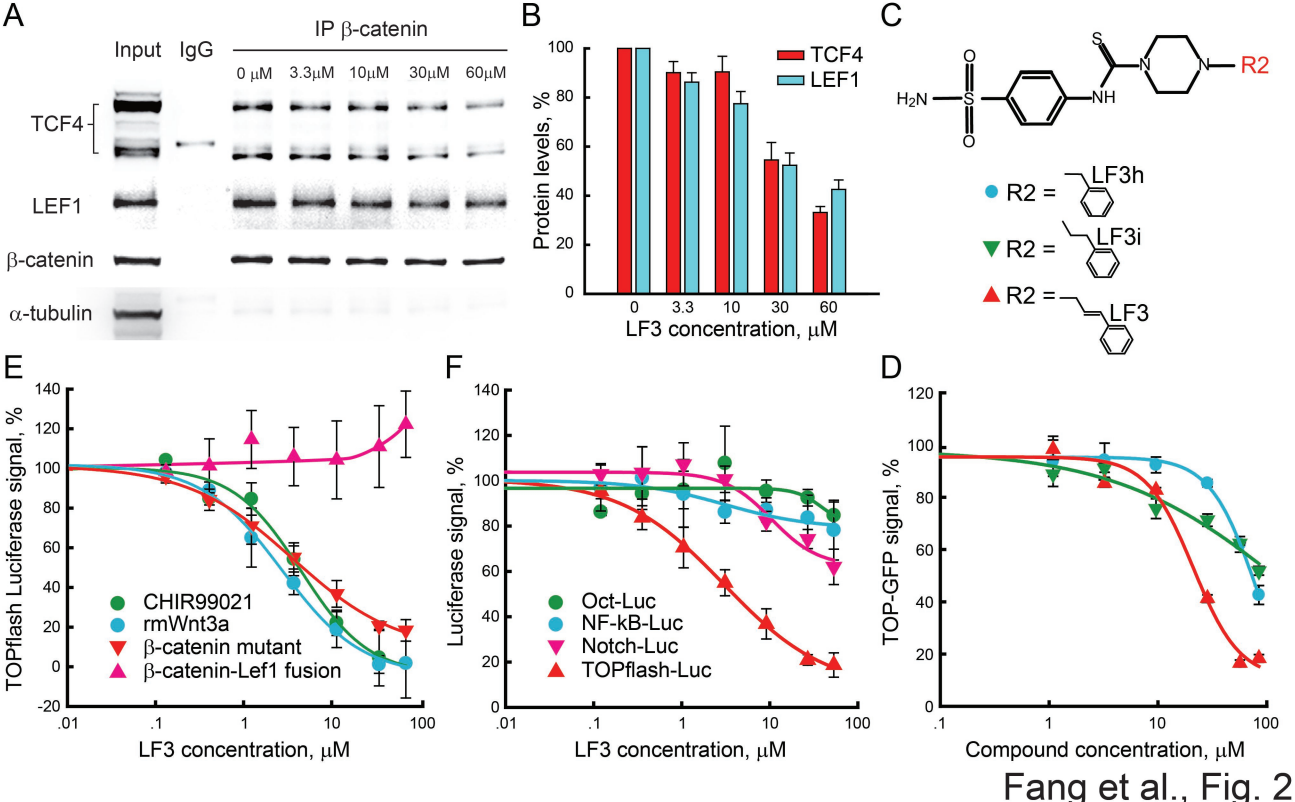

Fang et al., Fig. 2

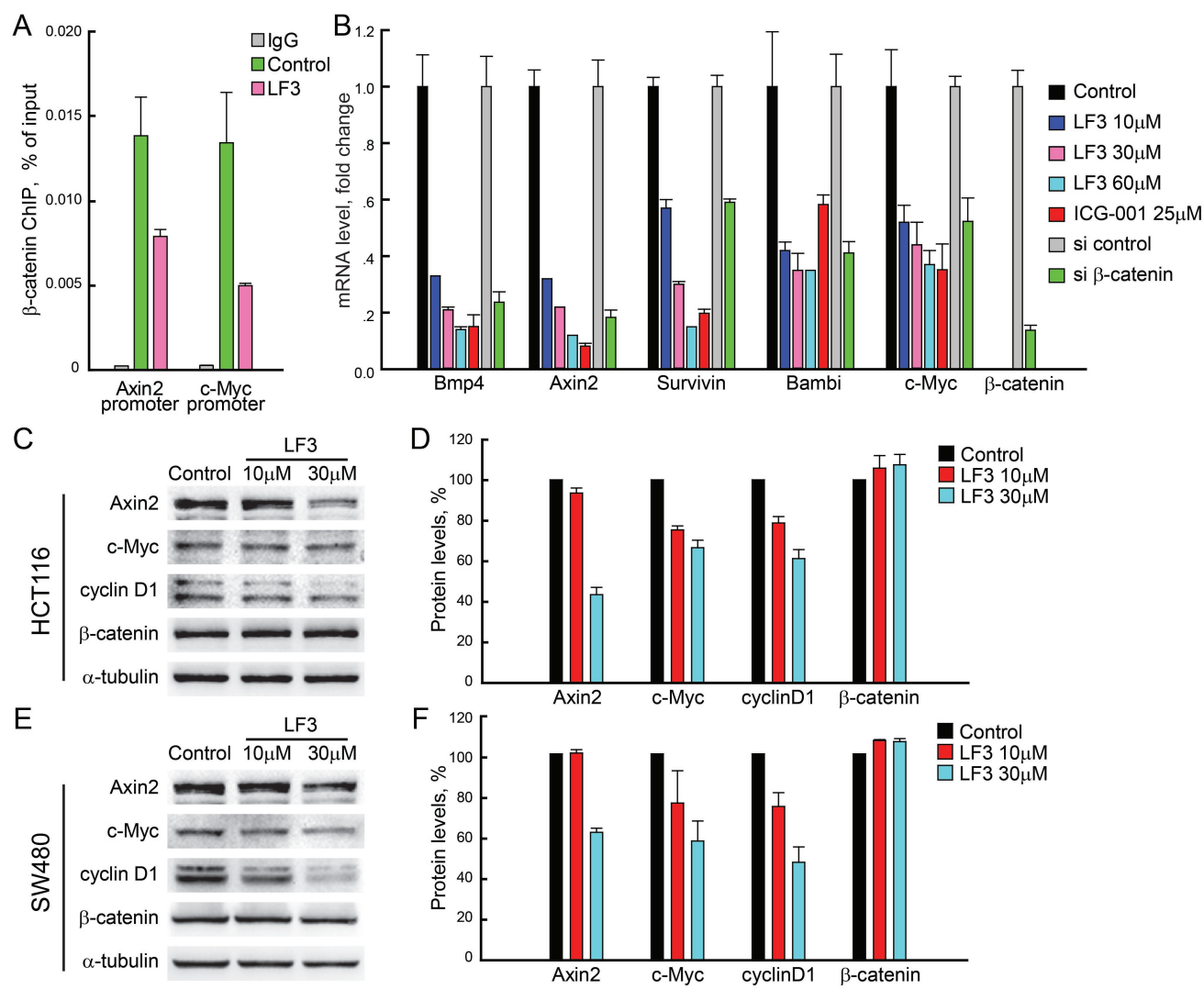

Fang et al., Fig. 3

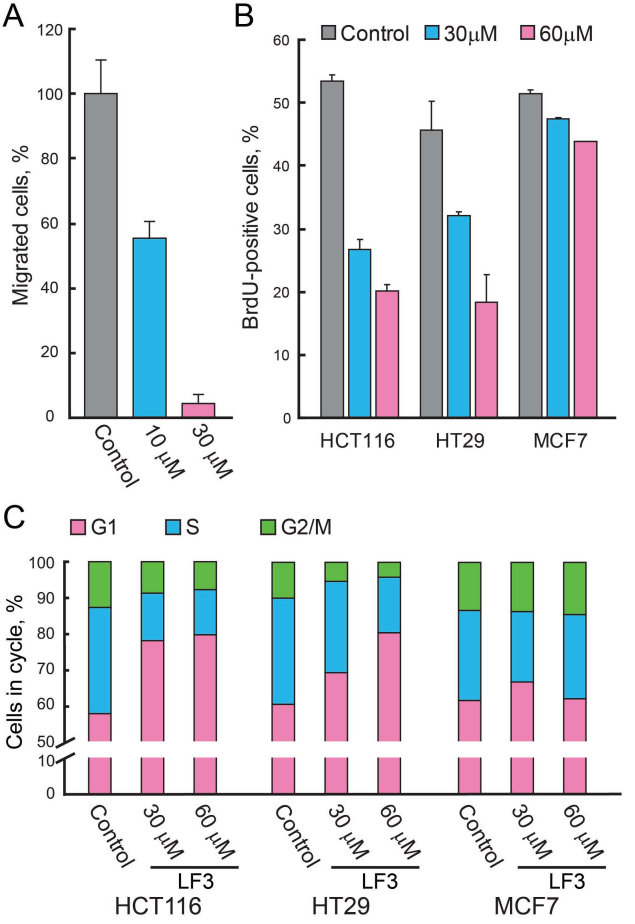

Fang et al., Fig. 4

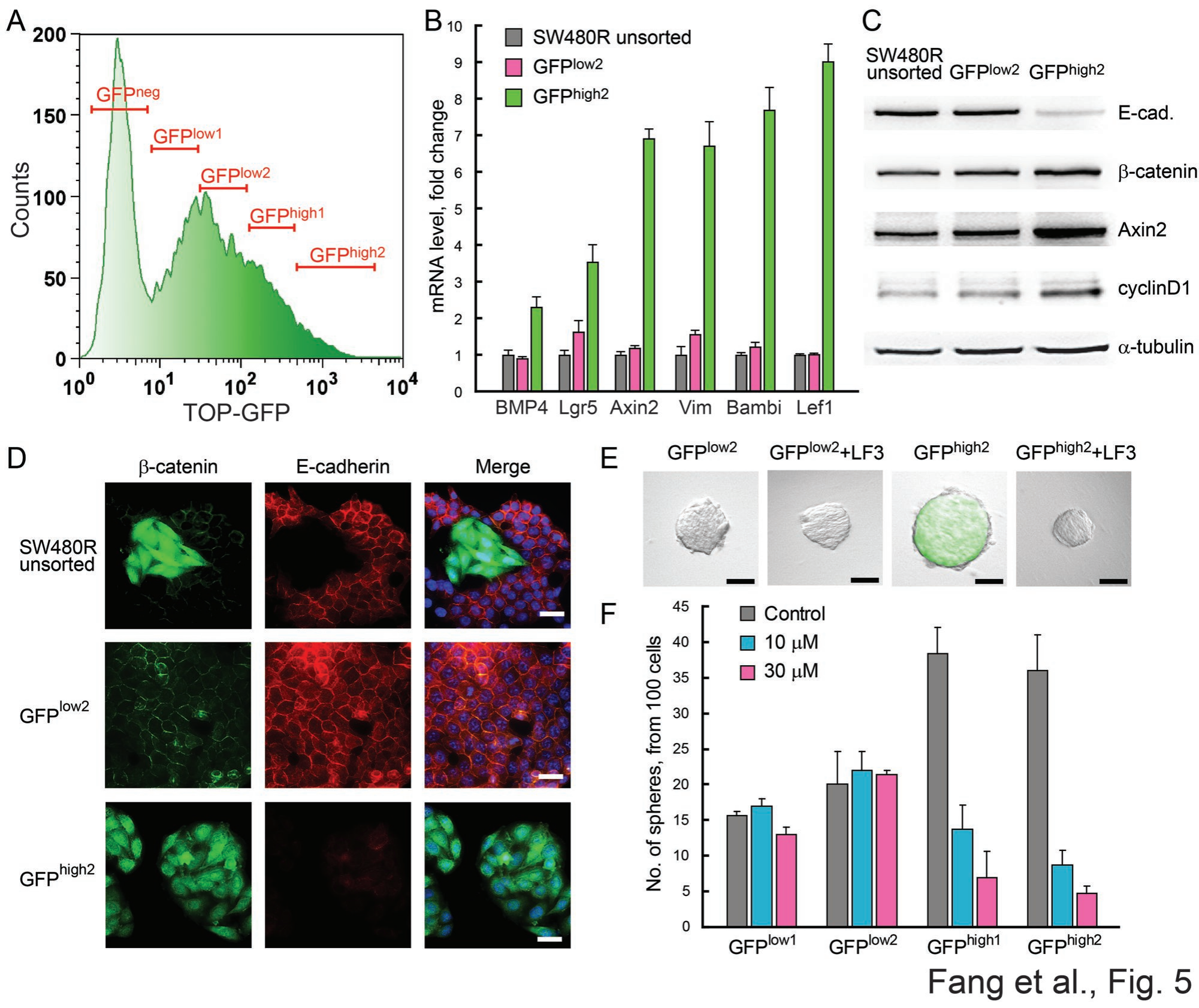

Fang et al., Fig. 5

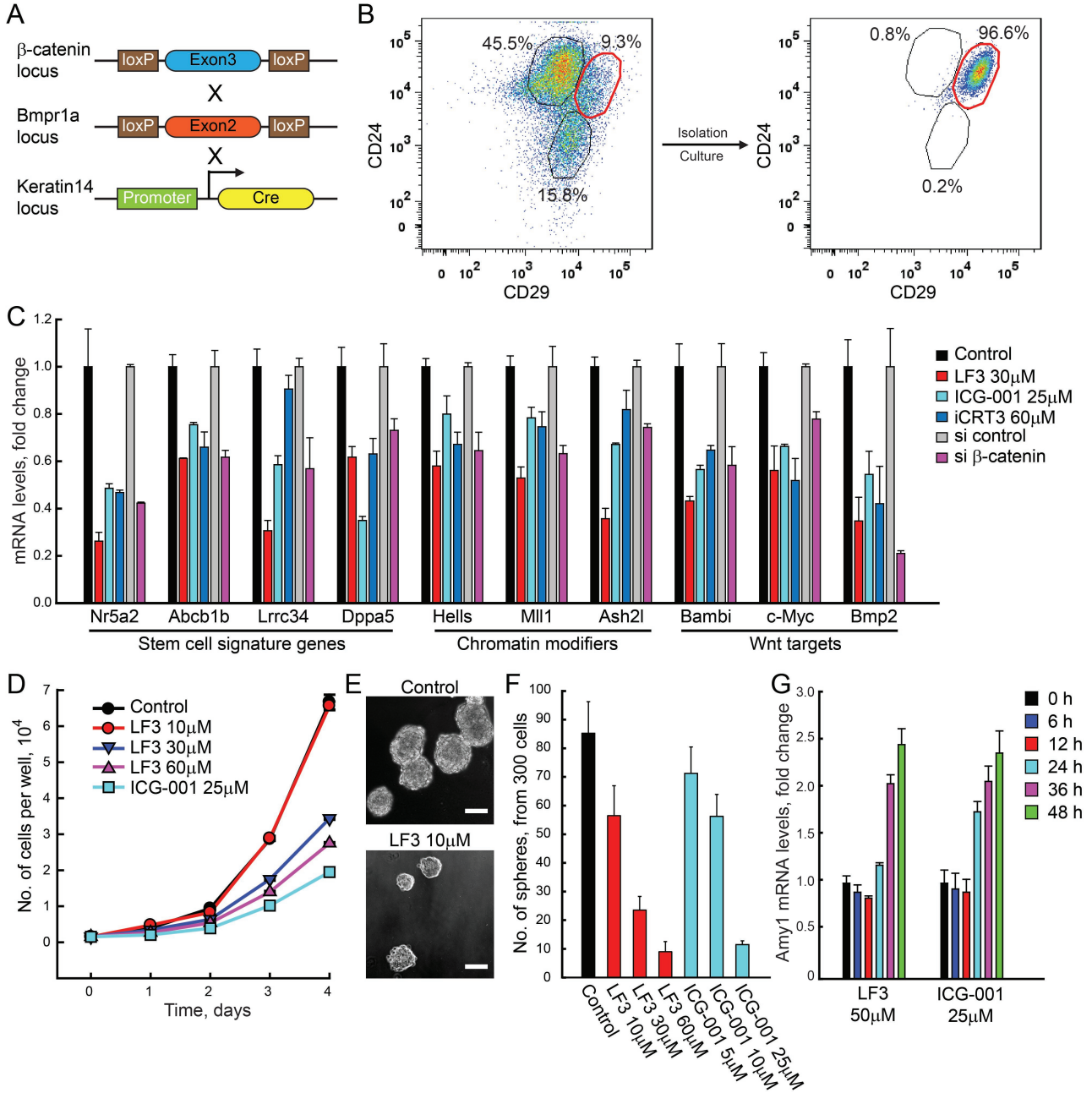

Fang et al., Fig. 6

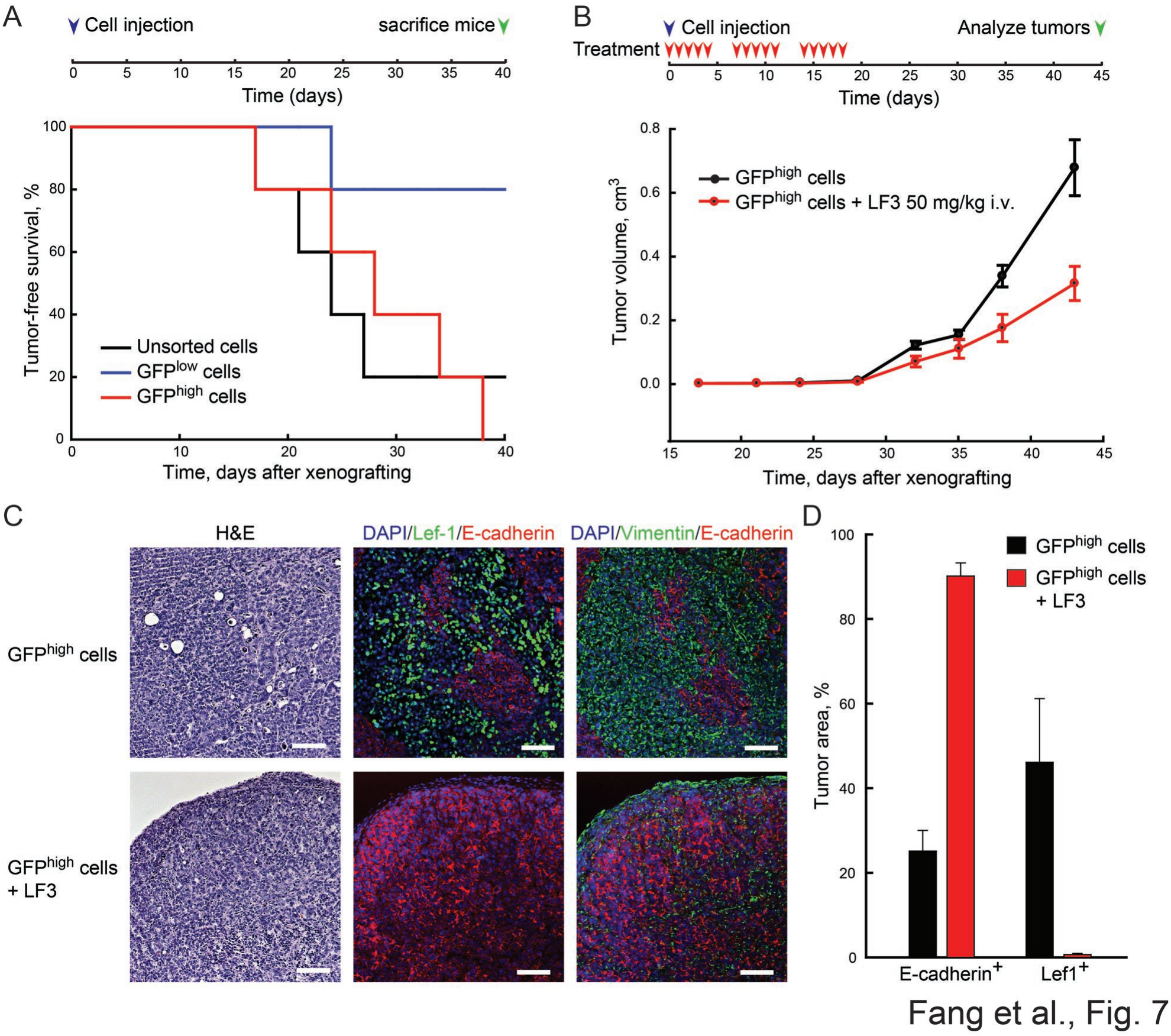

Fang et al., Fig. 7

Supplementary Material – Portions of Materials and Methods and Supplementary Figure Legends

Materials and Methods

Protein purification

GST-hβ-catenin (amino acids, aa 134-668), His-hTCF4 (aa 1-79) and mutant His-hTCF4 (aa 1-79 containing D16A) were expressed in *E. coli* BL21 cells by IPTG induction, 1mM for 4 h. After induction, cells were sonicated and incubated in PBS containing 1% Triton X-100 for 30 min at 4 ˚C to release proteins from cells, and the cell debris was remove by centrifugation at 12,000 X *g* for 30 min at 4 ˚C. Cell lysates containing different recombinant proteins were loaded on GSTrap FF and HisTrap FF columns (GE), respectively. GSTrap FF columns were washed with PBS, and HisTrap FF columns were washed with PBS containing 0.5 M NaCl and 40 mM imidazole. After washing, GST-hβ-catenin was eluted with PBS containing 10 mM reduced glutathione, and His-hTCF4 and His-hTCF4 (D16A) were eluted with PBS contianing 500 mM imidazole. Purified proteins were dialyzed with PBS containing 1 mM DTT and 20% glycerol overnight at 4 ˚C to remove reduced glutathione and imidazole, and stored at -80 ˚C.

ELISA

Nunc-immuno maxisorp 96 well plates (NUNC) were coated with purified His-hTCF4 in coating buffer (50 mM carbonate-bicarbonate, pH 9.6) overnight at 4 ˚C, blocked with 1% BSA in PBS for 1 h, washed with PBS containing 0.05% Tween-20, and incubated with purified GST-hβ-catenin in the presence of series of concentrations of various purified proteins or compounds. Concentrations of purified His-hTCF4 and GST-hβ-catenin used in the ELISAs

were determined by titration. Concentrations, which gave signals in linear range were chosen. To detect bound GST-hβ-catenin, plates were washed and incubated sequentially with anti-GST antibody (sc-101524, Santa Cruz) and HRP-conjugated anti-mouse antibody (715-035-150, Jackson ImmunoResearch laboratories), and measured with 1-Step Ultra TMB-ELISA (Thermo scientific) at 450 nm with a microplate reader Genios (Tecan).

Establishment of TOP-GFP reporter cell lines

The lentivirus particles (SABiosciences) encoding GFP under the control of a basal promoter element (TATA box) joined to tandem repeats of a consensus TCF/LEF binding site were transfected into HEK293 and SW480 cells. Stable clones were selected by puromycin (2 μg/ml) treatment. Next, fluorescence-activated cell sorting (FACS) was performed to select HEK293 reporter cells that were sensitive to CHIR99021 (3 μM, Axon Medchem) treatment, and the different populations of SW480 reporter cells were separated based on their GFP intensity.

Luciferase reporter assay

Plasmids encoding a firefly luciferase reporter-gene under the control of different responsive elements were transfected into Hela cells with a pRL-SV40 normalization reporter plasmid using Lipofectamine 2000 (Invitrogen). After desired treatments, cells were harvested in the passive lysis buffer (Promega), and 15 μl cell lysates were transferred to 96-well LumiNunc plates (Thermo Scientific). Firefly luciferase and Renilla luciferase were detected with D-luciferin buffer (75 mM Hepes, 4 mM $MgSO_4$, 20 mM DTT, 100 μM

EDTA, 0.5 mM ATP, 135 µM Coenzyme A, 100 µM D-Luciferin sodium salt, pH 8.0) and coelenterazine buffer (15 mM Na4PPi, 7.5 mM NaAc, 10mM CDTA, 400 mM Na_2SO_4, 25 µM APMBT and 1.1 µM coelenterazine, pH 5.0), respectively, using the CentroXS LB960 lumiometer (Berthold Technologies).

Co-immunoprecipitation

HCT116 cells were lysed in Co-IP buffer containing 50 mM Tris, pH7.5, 150 mM NaCl, 0.2% NP-40, 10% Glycerol, 1 mM DTT and 1 mM PMSF. Cell lysates were pre-cleaned by protein G sepharose beads (GE Healthcare) at 4 °C for 1 h. Pre-cleaned lysates were sequentially incubated with anti-β-catenin antibody (610154, BD) at 4 ˚C overnight and subsequently with protein G sepharose beads for an additional 1 h. The beads were then washed, incubated with series of concentrations of LF3 for further 1 h and washed again. All the washing and incubation steps were carried out in Co-IP buffer. The bound proteins were eluted by boiling in SDS sample buffer and analyzed by Western blotting.

Western blotting

Protein samples were loaded onto 8-12% SDS-pages (separating gel: 8-12% acrylamide, 0.32% N,N´-Methylbisacrylamide, 375mM Tris, pH 8.8, 0.1% SDS, 0.1% APS, 0.1% TEMED; stacking gel: 4% acrylamide, 0.1% N,N´-Methylbisacrylamide, 125 mM Tris, pH 6.8, 0.1% SDS, 0.1% APS, 0.1% TEMED) and separated in electrophoresis running buffer (25 mM Tris, 20mM glycine, 2% SDS). Separated proteins were transferred onto PVDF membranes in the transfer buffer (25 mM Tris, 192 mM glycine, 3% SDS, 10%

methanol). Non-specific binding of proteins on the membranes was blocked for 1 h at room temperature (RT) with blocking solution (4% BSA, 0.1% Tween20 in PBS) with constant shaking. The primary antibodies were diluted in blocking solution and incubated with the membranes at 4°C overnight with constant shaking. After washing in PBST (0.1% Tween20 in PBS), the membranes were incubated with HRP-conjugated secondary antibodies diluted in blocking solution for 1 h. After washing three times in PBST, the immuno-reactive bands were visualized with Western lightning chemiluminescence reagent plus (PerkinElmer) and Vilber Lourmat imaging system SL-3. Anti-TCF4 antibody (2953, Cell signaling) and anti-E-cadherin antibody (610181, BD) were used to analyze protein samples from Co-IP experiments. To evaluate Wnt target accumulation in HCT116 and SW480 cells, cells were treated with LF3 at the indicated concentrations for 24 h and lysed in RIPA buffer (50 mM Tris, pH8.0, 1% NP-40, 0.5% deoxycholate, 0.1% SDS, 150mM NaCl). Axin2, cyclin D1 and c-Myc were detected using anti-Axin2 (2151, Cell signaling), anti-cyclin D1 (sc-718, Santa Cruz) and anti-c-Myc (sc-40, Santa Cruz) antibodies, respectively.

Immunofluorescence

MDCK and SW480 cells were cultured on 8-well CultureSlides (BD). After desired treatments, cells were fixed with 4% formaldehyde in PBS for 15 min, and blocked in PBS with 1% BSA and 0.3% Triton X-100 for 1 h. Slides were then sequentially incubated with anti-β-catenin and anti-E-cadherin primary antibodies at 4 ˚C overnight, and fluorchrome-conjugated secondary antibody at RT for additional 1h. After washing with PBS, slides were covered with

Immunomount (Thermo Scientific), and the fluorescence images were recorded using Axio imager.Z1m and AxioCam MRm (Carl Zeiss).

Chromatin immunoprecipitation

After treating with LF3 for 4 h, HCT116 cells were fixed with 1% formaldehyde in PBS and incubated in swelling buffer (25mM Hepes, pH7.9, 1.5mM $MgCl_2$, 10mM KCl, 0.1% NP-40, 1mM DTT and 0.5mM PMSF) to prepare for extraction of nuclei. Afterwards, chromatin was sheared by sonication in sonication buffer (50mM Hepes, pH7.9, 140mM NaCl, 1mM EDTA, 1% Triton X-100, 0.1% Na-deoxycholate, 0.1% SDS and 0.5mM PMSF) and incubated with 2 µg of anti-β-catenin antibody (610154, BD) and 25 µl Dynabeads Protein G (100-03D, Life Technologies) over night at 4°C. The beads were washed successively with 1 ml sonication buffer, 1 ml high salt buffer (same as sonication buffer except 500 mM NaCl) and 1 ml LiCl wash buffer (20 mM Tris, pH 8.0, 1 mM EDTA, 250 mM LiCl, 0.5% NP-40, 0.5% Na-deoxycholate, 0.25 mM PMSF). All washing steps were repeated twice and performed on a rotating wheel at 4°C. Chromatin was eluted with elution buffer (50 mM Tris, pH 8.0, 1 mM EDTA, 1% SDS, 50 mM $NaHCO_3$) and purified with PCR purification kit (28104, Qiagen). Enriched chromatin regions were characterized by quantitative real time PCR (qRT-PCR).

Table S1. Primer sequences for ChIP experiment

Chromatin region	Primer	Sequence
Axin2 promoter	F	TCTGGTAGCATTATGGCCATCGCA
	R	AAAGTCCTCCAAGCCCAAATTCCC
c-Myc promoter	F	AATTAAACGTCCGGTTTGTCCGGG
	R	AAGGTGCTAGACGGGAGAATATGG

Gene transcription analyses with qRT-PCR

After desired treatments, cells were lysed in TRIzol, and mRNA was extracted according to the standard TRIzol protocol (Invitrogen). RNA concentrations and purities were determined by the Nanodrop ND1000 spectrophotometer (Thermo Scientific). To reverse transcribe mRNA into cDNA, M-MLV reverse transcriptase (Promega) and random primers (Invitrogen) were used with 5μg of total RNA, following the manufacturer's protocol. qRT-PCR was performed in a iQ5 Multicolor Real-Time PCR Detection System (Bio-Rad) using 10 μl 2X SYBR® Green (Thermo scientific), 0.5μl cDNA and 0.5μl of 10μM primer mixes. The primers were designed as to have an annealing temperature of 60°C and an amplicon length of 100-200bp in the following program (95°C 15 min; 94°C 20 sec, 60°C 45 sec, 72 °C 10 sec; 40 cycles).

Table S2. Primer sequences for qRT-PCR

Species	Gene	Primer	Sequence
Human	Bmp4	F	TCTATGTGGACTTCAGCGATGTGG
		R	AATTGACCAGGGTCTGCACAATGG
	Axin2	F	TCAAGTGCAAACTTTCGCCAACCG
		R	TGGTGCAAAGACATAGCCAGAACC
	Survivin	F	AGCCCTTTCTCAAGGACCACC

		R	CTTGAAGCAGAAGAAACACTGGGC
	Bambi	F	ATTCGATGCTACTGTGATGCTGCC
		R	ATTCCAATGTGGGTATGGTGGTGC
	c-Myc	F	TCTCCACACATCAGCACAACTACG
		R	TGTGTTCGCCTCTTGACATTCTCC
	β-catenin	F	TTCGAAATCTTGCCCTTTGTCCCG
		R	AATTCGGTTGTGAACATCCCGAGC
	Lef1	F	ACCTCAGGTCAAACAGGAACATCC
		R	AGTACACTCAGCAACGACATTCGC
	Lgr5	F	TGCTTACCAGTGCTGTGCATTTGG
		R	TGCACTGAATGAAGGGCTTTCAGG
	β-actin	F	GCATCCACGAAACTACCTTCAACTCC
		R	TTGATCTTCATTGTGCTGGGTGCC
Mouse	Nr5a2	F	GGGGCAGAAATAAGTTTGGGC
		R	TTGGAGGCGGAATGAATGTTC
	Abcb1b	F	TTATGCTGCTTGTTTCCGGTTCGG
		R	TTTGGCTTTCGCATAGTCAGGAGC
	Lrrc34	F	TCAAGGGAATAAACCTGAACCGGC
		R	ATTGCAGCTGACATCAAGGTAGCG
	Dpp55	F	GAAATATCTGTTTGGCCCACAGGG
		R	GCCATGGACTGAAGCATCCATTTAGC
	Hells	F	TTCGGAAATGTAATGGACAGC
		R	GGGCCACATACAAGAAAAGG
	Mll1	F	AACAAGCATGGATCTCCCAATGCC
		R	ACATGTAGCAACCAATGCCCTTGC
	Ash2l	F	AAATGGTGTCAATCAGGGTGTGGC
		R	ACATCAGCCAGTGTGTGTTCTACC
	Bambi	F	ATCAGCATGACAGCAGCAGAAACC
		R	TCTTGGAATGGTGTCCGTGAAAGC
	c-Myc	F	TCCTGAAGCAGATCAGCAACAACC

	R	TGCTTGAATGGACAGGATGTAGGC
Bmp2	F	TGTCTTCTAGTGTTGCTGCTTCCC
	R	TGAGCAGCCTCAACTCAAATTCGC
β-actin	F	TCGTGCGTGACATCAAAGAGAAGC
	R	ATGGATGCCACAGGATTCCATACC

Proliferation analyses with BrdU

HCT116, HT29 and MCF7 cells were treated with indicated concentrations of LF3 for 24 h. 3-6 h before collecting cells, 10 μM BrdU was added into the culture medium. After trypsinization, single cell suspensions were fixed in 70% ethanol on ice for 30 min, treated with 2 M hydrochloric acid at RT for 30 min, and sequentially incubated with anti-BrdU antibody (ab6326, Abcam) and DyLight488-conjucated anti-rat antibody (712-485-150, Jackson ImmunoResearch laboratories) in PBS with 0.2% Tween-20 and 1% BSA. BrdU-positive cells were detected by the FACSCalibur system (BD).

Cell migration assays

Cell motility was assessed using 24-well transwells (pore diameter: 8 μm, Corning). SW480 cells were seeded in the upper chamber in serum-free DMEM with 0.1% BSA. 20% serum was supplemented to medium in the lower chamber. After incubation with different concentrations of LF3 for 24 hours at 37°C, nonmigrant cells were scraped off using a cotton swab, and the migrated cells on the filters were stained with crystal violate, photographed and counted.

Cell death and apoptosis analyses

HCT116 cells were treated with 60 μM LF3 or 1μg/ml puromycin for 24 h, and then trypsinized to single cell suspensions. Fresh cells were incubated with 5 μg/ml propidium iodide (Sigma) in PBS for 10 min and analyzed for accidental cell death using the FACSCalibur system (BD). For the apoptosis analyses, cells fixed with 3% formaldehyde were sequentially incubated with anti-cleaved-caspase3 antibody (9661, Cell signaling) and DyLight488-conjugated secondary antibody (711-485-152, Jackson ImmunoResearch laboratories) in PBS with 0.5% BSA. The percentage of cleaved-caspase3-positive cells was analyzed by the FACSCalibur system (BD).

Cell cycle analyses

HCT116, HT29 and MCF7 cells were treated with the indicated concentrations of LF3 for 24 h, trypsinized to make single cell suspensions and fixed in 70% ethanol overnight. After washing with PBS, cells were incubated in Propidium iodide (PI)-staining buffer (10mM Tris, pH7.5, 50 μg/ml PI, 5 mM $MgCl_2$ and 10 μg/ml Rnase A) at 37 °C for 30 min. DNA contents of cells were measured by the FACSCalibur system (BD) and analyzed by the software FlowJo (Tree Star).

Cell surface marker analysis

All cell surface markers were antibody-stained in PBS with 5% BSA for 15 min at RT. FITC conjugated anti-CD44 (55478, BD) and PE-Cy5 conjugated anti-CD29 (559882, BD) antibodies were used to characterize SW480 cells. PE-conjugated anti-CD24 (553262, BD) and Alexa700 conjugated anti-CD29

(102218, Biolegend) antibodies were used to analyze mouse salivary gland cancer stem cells.

Gene expression profiling

After desired treatments, total RNA of salivary gland CSCs were extracted according to the standard TRIzol protocol (Invitrogen). RNA was purified with RNeasy kit (Qiagen) and prepared with TotalPrep RNA amplification kit (Illumina) for the microarray analysis using MouseRef-8 v2.0 expression beadchip Kit. Microarray data (GEO accession: GSE73732) were analyzed and exported with the software Genome Studio (Illumina). Pearson correlation was calculated with http://www.wessa.net/rwasp_correlation.wasp. Expression clustering was calculated and visualized with software Cluster and TreeView (Stanford University), respectively. Functional clustering of interesting genes was performed with http://david.abcc.ncifcrf.gov/.

Supplementary Figure Legends

Fig. S1 Technology and protein production for the primary High Throughput Screen (HTS). (A,B) Schematic illustrations of AlphaScreen and ELISA with purified proteins. (C) Inhibition of the TCF4/β-catenin interaction in the presence of various recombinant fusion proteins in competitive ELISAs. (D) Schematic illustration of the screening process: 16,000 compounds were screened in the primary screen with the AlphaScreen technology; 18 out of 132 primary hits were validated in both AlphaScreen and ELISAs. (E,F) 5 hits (labeled LF1-5) showed an IC_{50} of less than 10 μM in both assays**.**

Fig. S2 Specific inhibition of Wnt signaling by LF3. (A) Scheme of simplified Wnt signaling and interfering compounds: CHIR99021 and XAV939 exert their agonistic and antagonistic effects, respectively, on the β-catenin destruction complex, while ICG-001 and LF3 inhibit Wnt signaling by targeting the transcription complex. (B) Inhibition of Wnt/β-catenin signals by different Wnt inhibitors: TOP-GFP reporter cells were treated with various concentrations of CHIR99021 and different Wnt inhibitors, LF3 (30 μM), ICG-001 (3 μM) or XAV939 (1 μM). (C) The pRL-SV40 plasmid was co-transfected with different reporter plasmids including TOPflasch-Luc, Oct-Luc, NF-κB-Luc or Notch-Luc into Hela cells. Different reporter activities were stimulated with specific treatments at different dosages. The dosages (arrowheads) that induced moderate activation of individual pathways were chosen to assess the effect of LF3 on these pathways. (D) MDCK cells were treated with 60 μM LF3 or 40 U/ml HGF, and fixed at 24 h to visualize the distribution of E-cadherin and β-catenin by immunofluorescence. Membrane co-localization of

E-cadherin and β-catenin remained unchanged in LF3-treated cells as in control cells, but it was significantly altered upon HGF treatment. (E,F) β-catenin was immunoprecipitated from protein extracts of HCT116 cells that were incubated with LF3 at increasing concentrations, and E-cadherin bound to β-catenin was not changed, as shown by Western blotting. (G) After 5 min treatment with trypsin, the protein levels of E-cadherin and β-catenin in MDCK cells were analyzed. (H) After trypsinization, MDCK cells were kept in complete medium to reform cell-cell adhesion. Cells were fixed at different time points for analyzing the distribution of β-catenin by immunofluorescence.

Fig. S3 Inhibition of Wnt signaling by LF3 in colon cancer cells. SW620 (A,B), HCT15 (C,D), SW48 (E,F) and LS174T (G,H) colon cancer cells harboring different mutations in canonical Wnt components were treated with LF3 for 24 h. Downregulation of Wnt targets at the protein level was demonstrated by Western blotting.

Fig. S4 LF3 doesn't cause apoptosis or cell death. HCT116 cells were treated with 60 μM LF3 or 1 μg/ml puromycin for 24 h and fixed for antibody staining of cleaved caspase3 (A), or freshly stained by PI (B) to observe cell membrane integrity.

Fig. S5 CSC markers and self-renewal of GFP^{high} SW480 cells. (A,B) SW480 cells were double-stained with antibodies against the CSC markers CD44 and CD29 and analyzed by flow cytometry. Two populations of cells, CD44^{high}CD29^{+} and CD44^{low}CD29^{+}, were observed. (C) The self-renewal of GFP^{high} cells was tested in sequential rounds of colony assays in the

presence of LF3. LF3 reduced the colony numbers continually in each passage.

Fig. S6 Influence of LF3 on gene profiling and differentiation of mouse salivary gland CSCs. (A) The differentiation markers CA6 and Loricrin of salivary gland CSCs were analyzed by qPCR after treatment with LF3. (B) Salivary gland CSCs were cultured in matrigel to form 3D structures. Undifferentiated structures (filled spheres) and differentiated structures (hollow spheres) were recorded and quantified after 14 days. (C) Salivary gland CSCs were treated with 30 μM LF3 or 25 μM ICG-001 for 24 h and collected to perform gene profiling using Illumina microarrays. The heat map of a panel of canonical Wnt targets demonstrated that LF3 and ICG-001 inhibited Wnt signaling, but showed slight differences in choosing their targets. (D,E) The overlap between genes downregulated by LF3 and ICG-001 and the "Pearson correlation coefficient" indicate the largely similar influence of LF3 and ICG-001 treatment on gene profiling. (F,G) Expression clustering revealed groups of genes that were differentially or similarly regulated by different compounds. Genes in different groups were studied by function clustering using the DAVID bioinformatics resources.

Fig. S7 LF3 reduces tumor growth without showing toxicity *in vivo*. (A) Mice xenografted with GFP^{high} SW480 cells were treated *i.v.* with vehicle (n=10) or 50mg/kg LF3 (n=6) for 3 weeks, and the tumor weight was measured on day 45. (B) Mice xenografted with GFPhigh SW480 cells were treated *i.v.* with vehicle (n=6) or 50mg/kg LF3 (n=6) after palpable tumors had

developed, and the tumor volumes were monitored over time. (C) The body weight of mice in control and treated groups was monitored over time. (D,E) Expression changes of KRT20 and MUC2 in LF3-treated tumors were examined by immunofluorescence and quantified. 10 tumors from the vehicle group and 6 tumors from the LF3 group were evaluated. (F) H&E staining of colon, small intestine and stomach of control and LF3-treated mice.

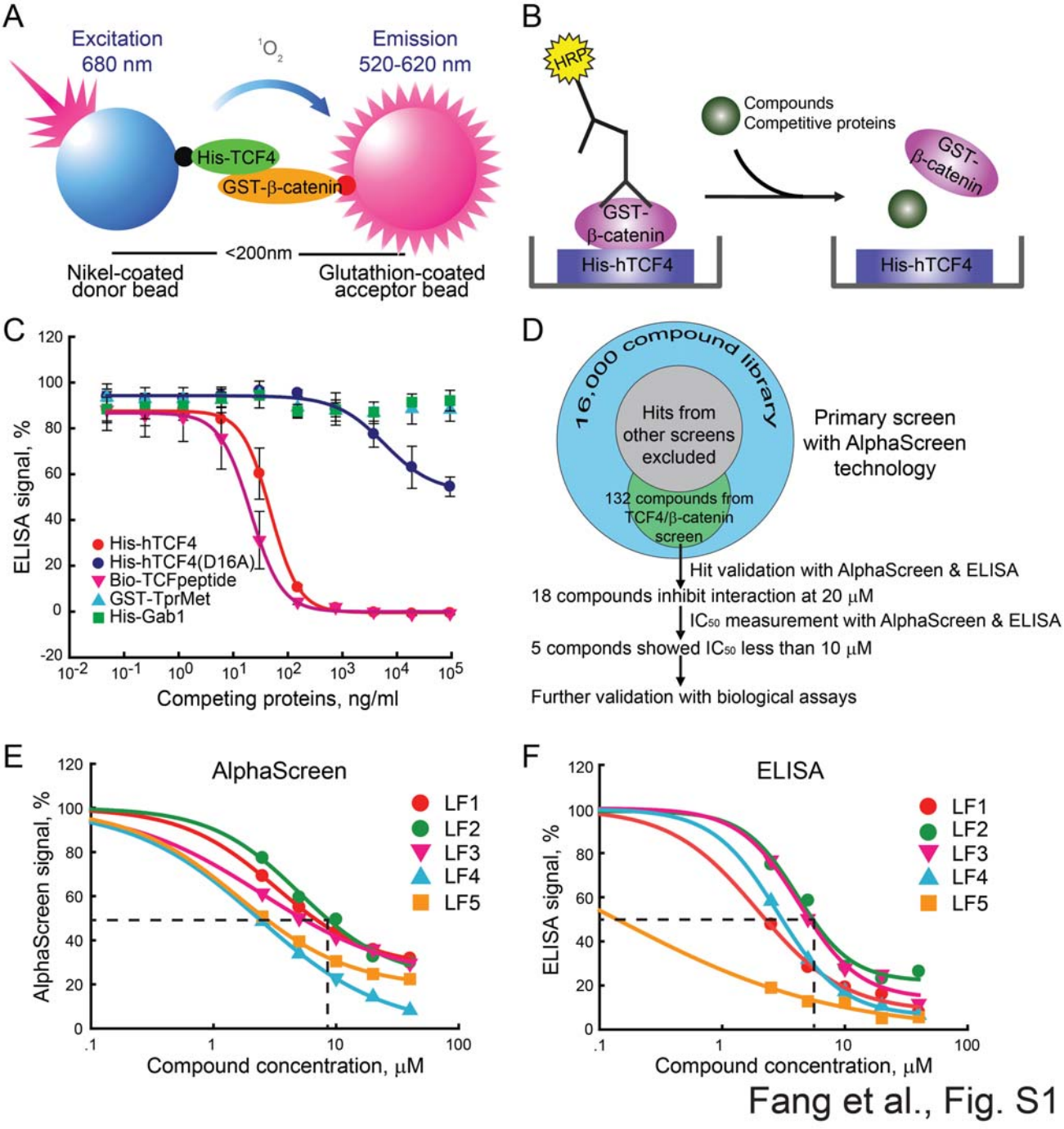

Fang et al., Fig. S1

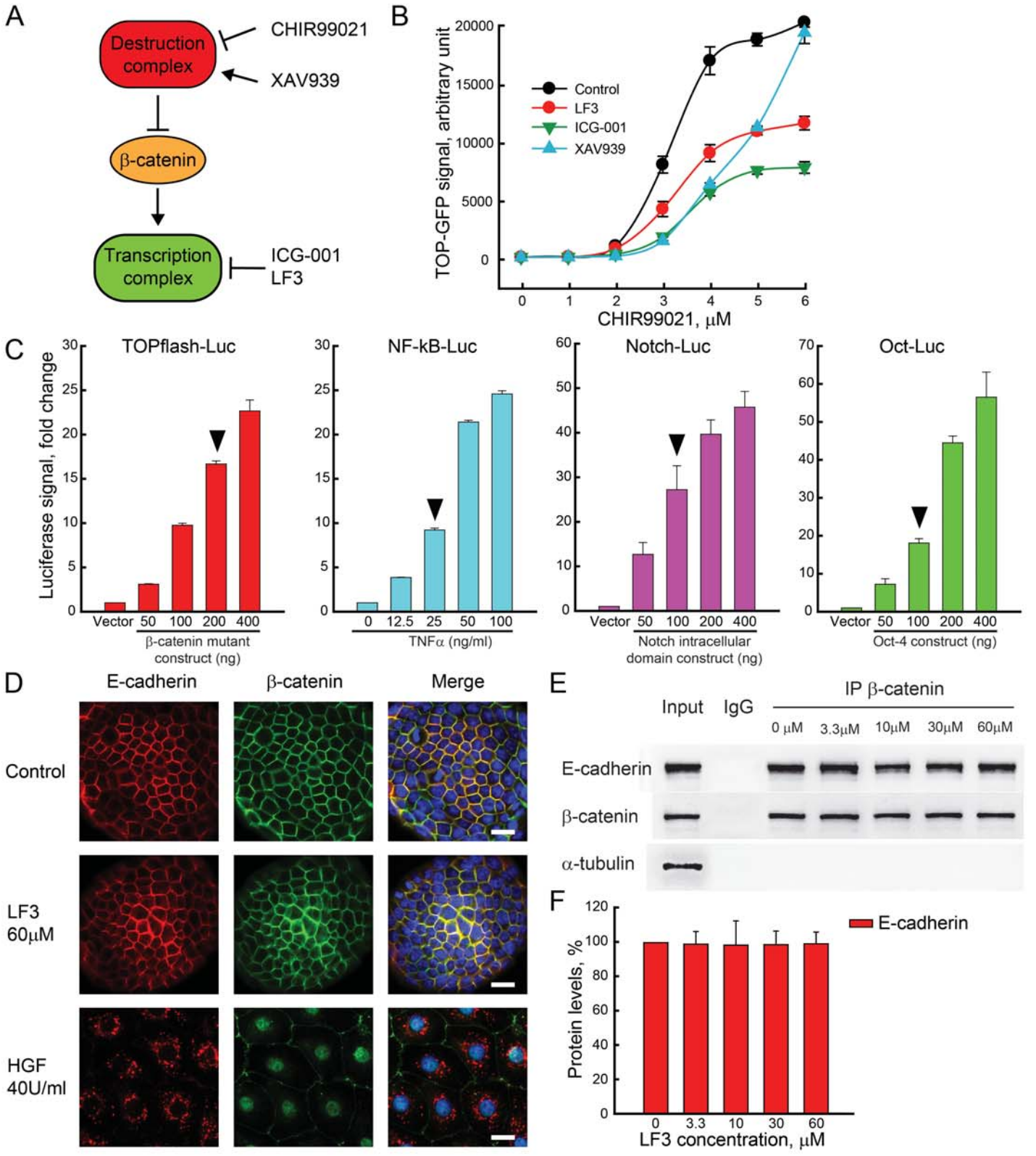

Fang et al., Fig. S2

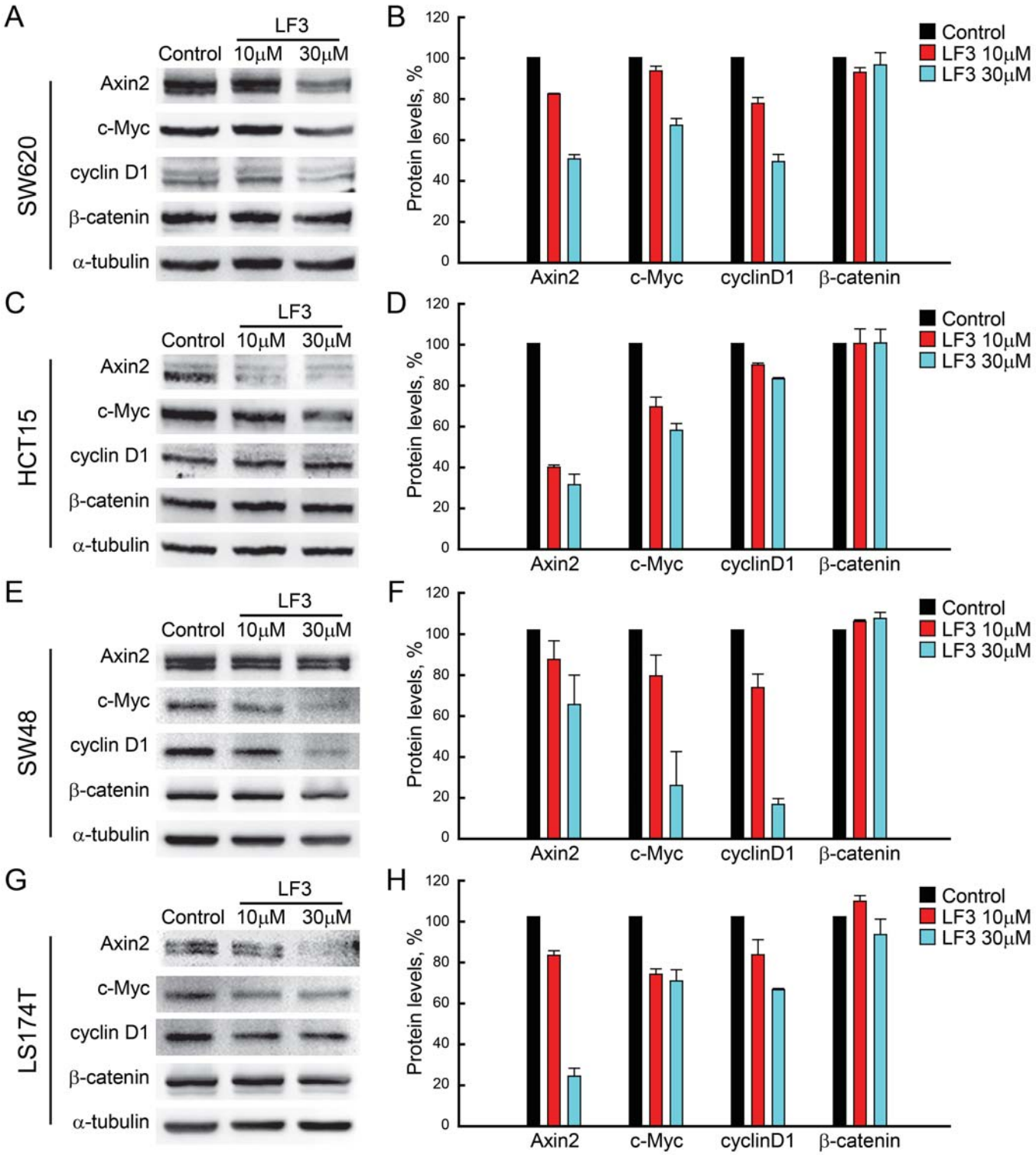

Fang et al., Fig. S3

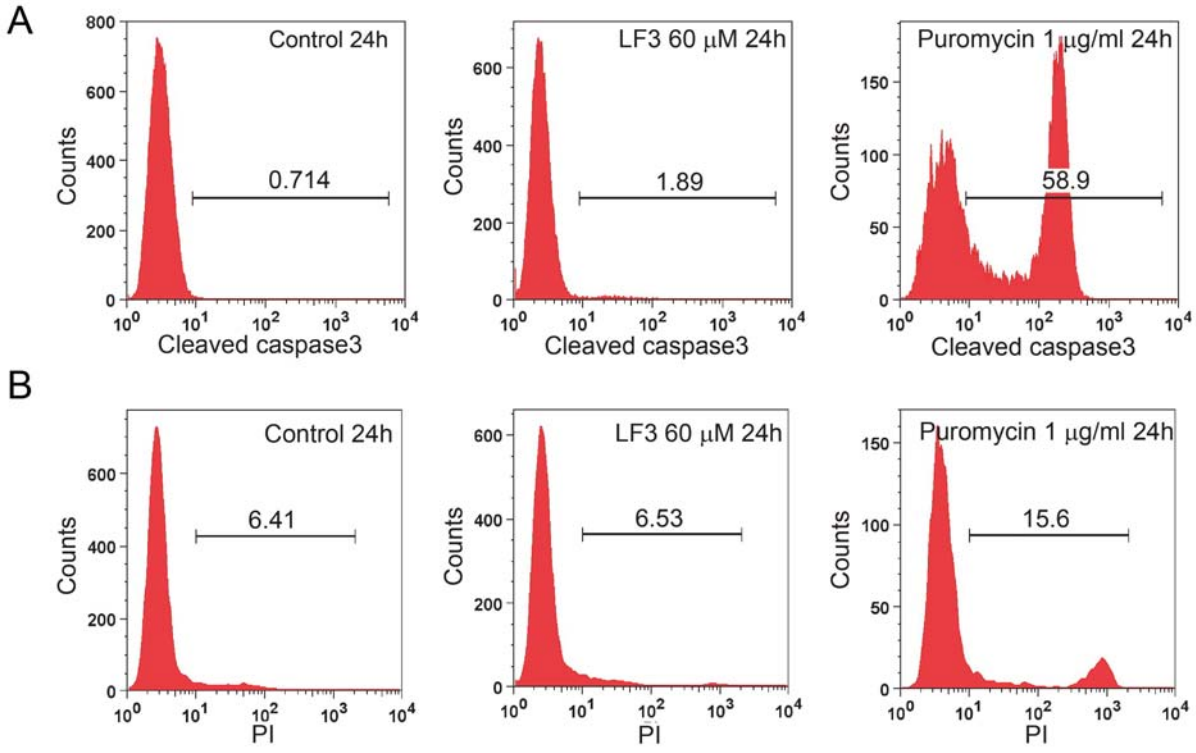

Fang et al., Fig. S4

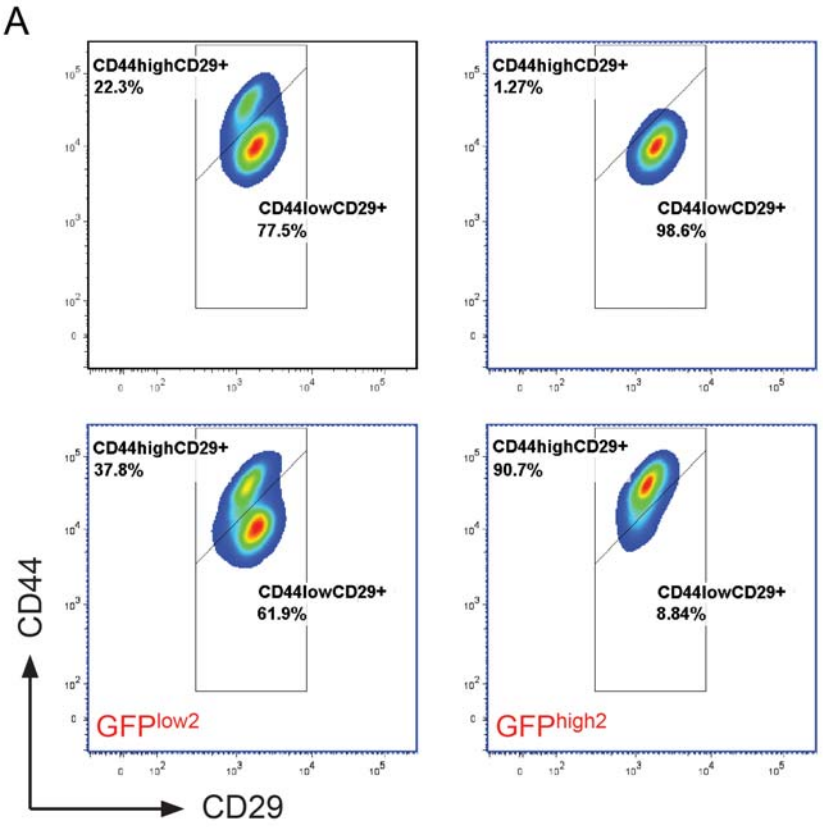

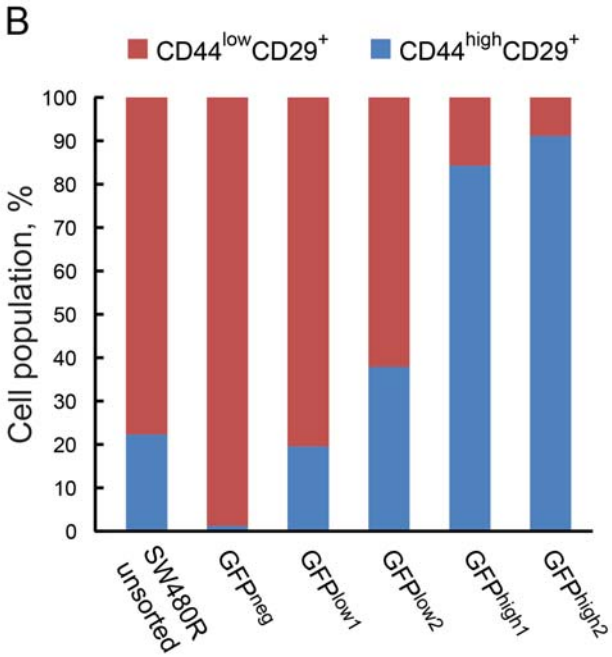

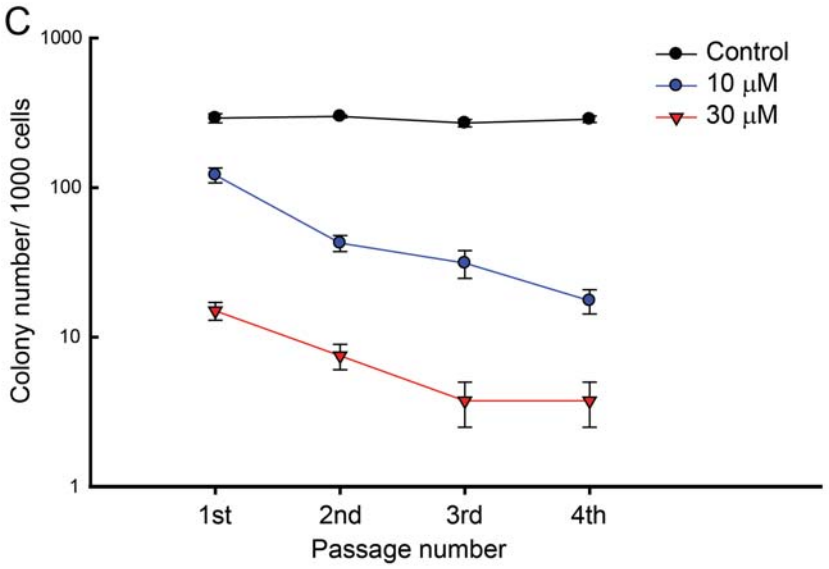

Fang et al., Fig. S5

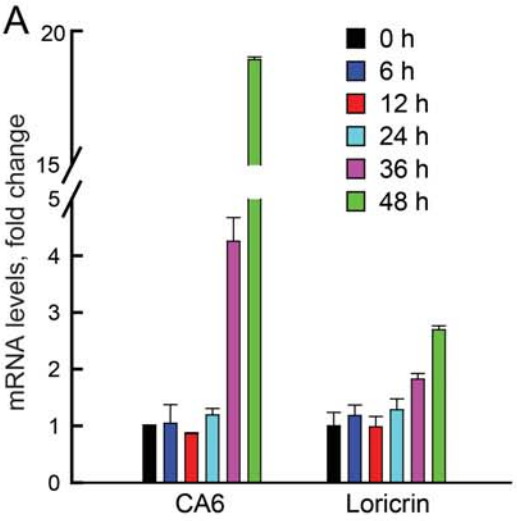

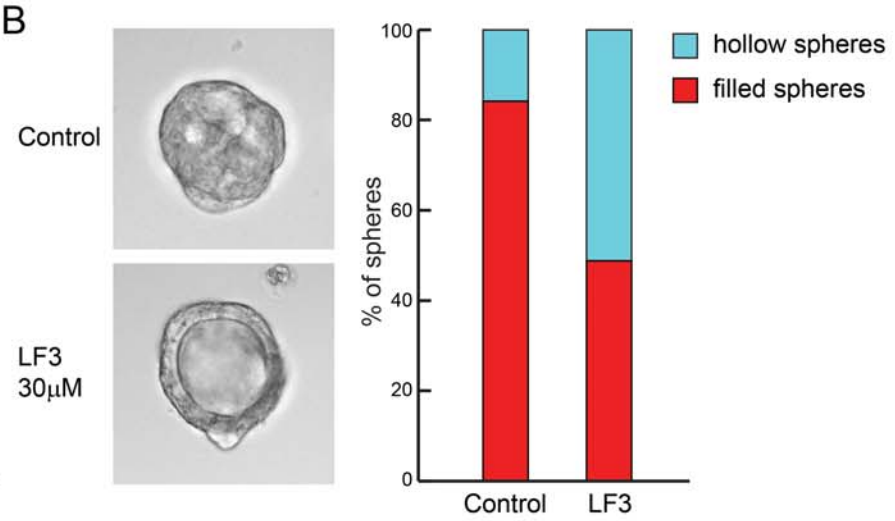

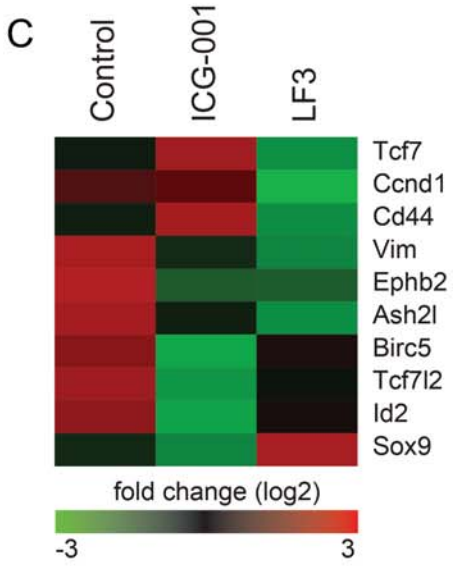

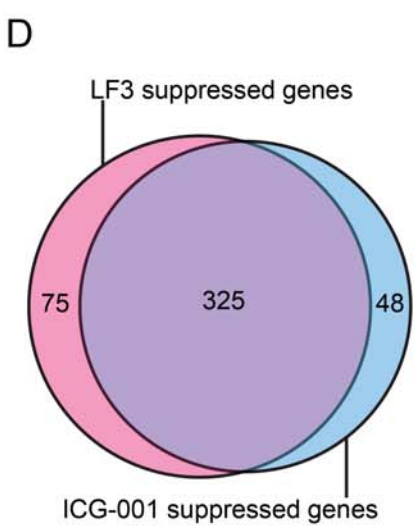

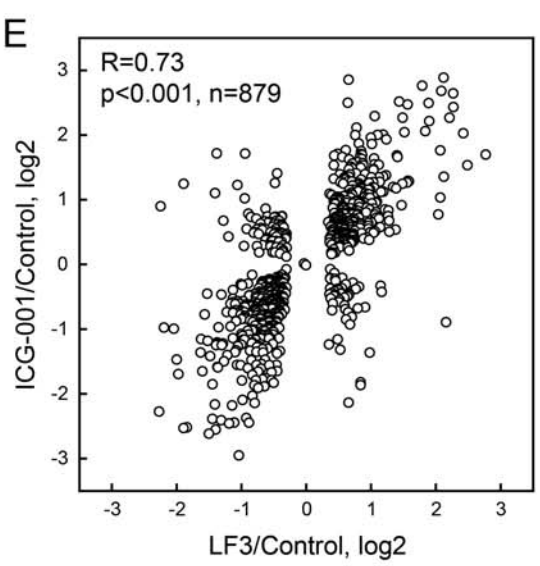

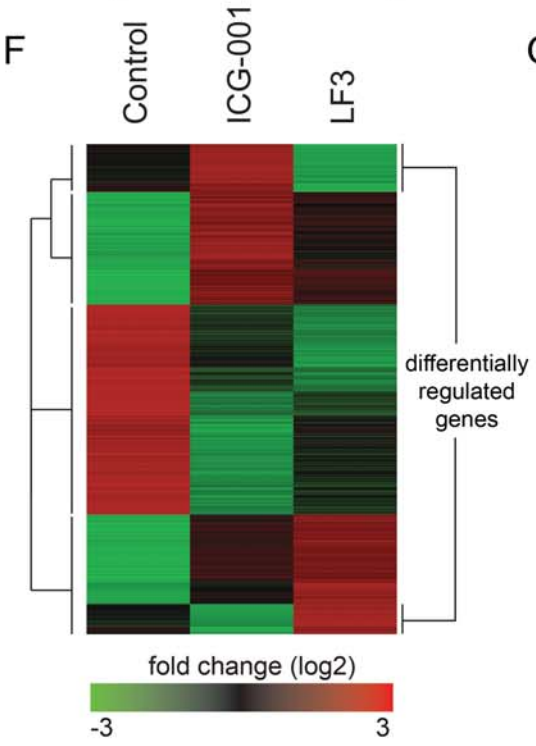

G

Regulation by ICG-001	Regulation by LF3	Fuctional clusters (No. of genes in the cluster)
Down	Down	cell cycle process (18); steroid metabolic process (8); transcription regulation (39); monosaccharide metabolic process (9); purine nucleotide binding (36); cellular response to stress (11); regulation of apoptosis (15); mRNA splicing (8)
Down	Up	metal ion binding (13)
Up	Down	purine nucleotide binding (13)
Up	Up	protein localization (25); mitochondrial envelope (15); cellular protein localization (13); membrane fraction (16); protein catabolic process (17); phosphate metabolic process (22); purine ribonucleotide binding (36); cytoplasmic vesicle (14); regulation of apoptosis (14)

Fang et al., Fig. S6

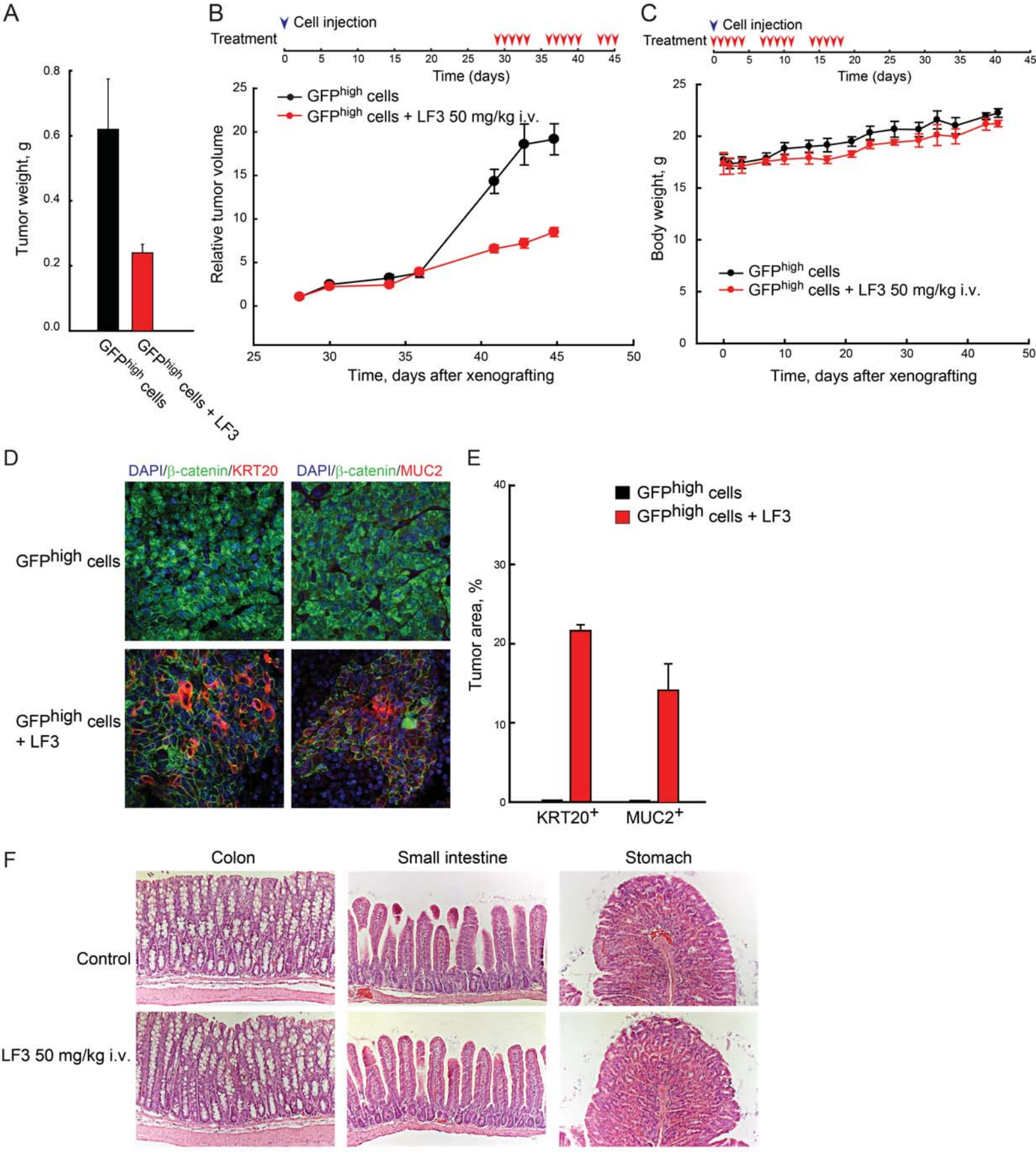

Fang et al., Fig. S7